Composition and source of the sediment in the kleine Noordwaard, Biesbosch Netherlands.

Source: aereal photograph 2008

Nanda Kik, 3539865
University Utrecht
First supervisor: M. van der Perk
Second supervisor: H. Middelkoop
July, 2015

Contents

Abstract

Tidal wetlands are an important environment for natural processes as well as human activities. They are, however, are rapidly disappearing. To preserve these wetlands, their morphological processes must be comprehended. The objective of this research is to determine the source of the sediment using the composition of the sediment. This will be accomplished by using different sampling and measuring methods. A total of four sampling methods are used: jars, containers, grass mats and freshly deposited sediment samples. Firstly, suspended sediment is caught in submerged jars in the channel. Secondly, tidally submerged containers and grass mats are placed on the soil for trapping suspended sediment. Lastly, freshly deposited sediment samples, submerged and above water level, were taken with a soil auger. Two fingerprinting technique are chosen, chemical fingerprinting using x-ray fluorescence and radiometric fingerprinting using activity concentration. The x-ray fluorescence measurements are statistically analysed to determine a weighted ratio.

Determined by the weighted ratio, it was discovered that of the 200 samples, 57 % of the deposited sediment which originated from the polder itself and 43 % originated from the river. The freshly deposited sediment thickness varied from 0 to 11.5 cm as did the spatial distribution on a small scale. The variance of the weighted ratio can for 86 ± 38% be accounted for by the unknown original composition of the sediment and for 14± 38% it can be accounted for by the regression analysis. The sediment composition of the area provides information about the sediment source. Only two main sources could be distinguished by composition calculations: recent sediment originating from the river Rhine or reworked sediment originating from the relatively older polder soil. When interpreted, more sources can be deduced: firstly, the sediment of the polder that was reworked. Secondly, the sediment originating from an older, more contaminated tidal creek that was found in the southern part of the area. Lastly, the sediment brought in for building activities to construct the current nature development habitat.

1 Introduction

The human population is located mainly at the coastal areas of the world with 18 of the world's 27 megacities and 61% of the world population located in that area ((Matsuura, et al., 2009) and (Bianchi, Allison, & Cai, 2013)). In fact, it is estimated that the world population living in the coastal area will have grown to 75% in 2025 (Bianchi, Allison, & Cai, 2013). Tidal wetlands in particular have always been favored by humans as living area due to advantages such as transport, drinking water and food. From nature's perspective, tidal wetlands are an important ecosystem due to the dynamics between land, river, ocean and the relatively large flora and fauna population (Bianchi & Allison, 2009). But tidal wetlands are increasingly vulnerable to flooding as a result of human interference in the natural dynamics (Syvitski, et al., 2009). A tidal wetland is a natural 'recorder' of global environmental changes, it builds out or drowns as a result of natural changes in the incoming sediment flux (Syvitski, et al., 2009), sea level changes, tectonics and outgoing sediment flux (Bianchi & Allison, 2009). Human interference such as land reclamation, land purpose changes and engineered constructions, has led to increasing subsidence rates and decreasing sedimentation rates, which has resulted in the drowning of the tidal wetlands. Expected is that combined with the predicted sea level rise this drowning effect will be enhanced even further ((Törnqvist, et al., 2008), (Asselen, 2010), (Syvitski, Vörösmarty, Green, & Kettner, 2005) and (Walling D. , 2006)).

Tidal freshwater wetlands are defined as: 'The landscape position of tidal freshwater wetland is at the upper end of the estuary where river discharge is sufficient to prevent intrusion of saline water but where tidal influence still extends' (Barendregt, Baldwin, & Whigham, 2009). Due to the economic and ecological importance of the tidal wetlands, research was instigated to come up with suitable measures to prevent tidal wetlands from drowning. Therefore quantitative knowledge of natural dynamics of tidal wetlands, water and sediment fluxes were needed. Monitoring in tidal freshwater wetlands continues to give more insight in the behavior of water dynamics, sediment fluxes and sedimentation patterns on a spatial and temporal scale, which can be used to understand the morphology of tidal wetlands (Barendregt, Baldwin, & Whigham, 2009).

Tidal wetlands are 'recorders' of environmental changes; the Netherlands have been the drain of North-western Europe from the Pleistocene onwards, resulting in a filling-up subsiding delta with Rhine and Meuse sediments (Figure 1) (Busschers, et al., 2005). Part of these sediments has been contaminated with heavy metals by the industrial waste from the 19th century onwards. In the southwest of this Rhine-Meuse delta a small inland tidal wetland is situated, which is called the Biesbosch. It is connected to the sea by the Haringvliet barrier and is downstream from the river Rhine and Meuse. In the Biesbosch, in a former agricultural polder called the 'kleine Noordwaard', the dikes have been removed and therefore it has become a natural tidal wetland through which Rhine water is flowing.

Due to the depoldering of the 'kleine Noordwaard' in 2008, it is the perfect area for an integrated research on quantification of factors and mechanisms that control the sediment budget of a delta system and to assess the impact of changing sediment budgets on the development of drowning delta under climate change, rising sea level and changing river peak discharges. The outcomes of this research will be used to make robust scenarios for the management plan of the area and to increase the knowledge of delta dynamics.

So in this study area, this research will try to determine the origin of the sediment found. The origin of sediment was traditionally discovered by ascertaining the local sediment budget. The local sediment budget was determined by direct measurements with erosion pins, profilometers and visual observations ((cf Wilson et al. 1993; McCool et al 1981; David and Gregory 1994; Loughran et al. 1992 in (Walling & Collins, 2002)). These direct measuring methods have a relatively small spatial and/or temporal sampling range and are therefore labor intensive and expensive. This technique however cannot be used to reconstruct historical sediment sources since. Due the large time frame deposition of sediment in the study area, a more fitting technique is fingerprinting, which is suitable for ascertaining historical as well as current sediment sources and less costs are involved ((Peart & Walling, 1988); (Loughran, Campbell, & Elliott, 1982); (Hebink, Middelkoop, Van Diepen, Van der Graaf, & de Meijer, 2007)). The fingerprinting technique also makes it possible to determine the relative importance of the major sediment sources ((e.g. Wall and Wilding, 1976; Wood, 1978; Oldfield et al., 1979 in (Peart & Walling, 1982)). Over the past 20 years this technique has been performed to determine the sediment source by finding a single diagnostic property: mineralogical, colorimetric, mineral-magnetic, chemical, organic, radiometric, isotopic and physical fingerprinting (Collins, Walling, & Leeks, 1988). But with a single sediment property the risk of false or coincidence sediment-source matches increases so the search for a combination of properties has been said to be the most reliable (Collins & Walling, 2002). The fingerprinting technique is now used in marine, fluvial and glacial environments (Hebink, Middelkoop, Van Diepen, Van der Graaf, & de Meijer, 2007).

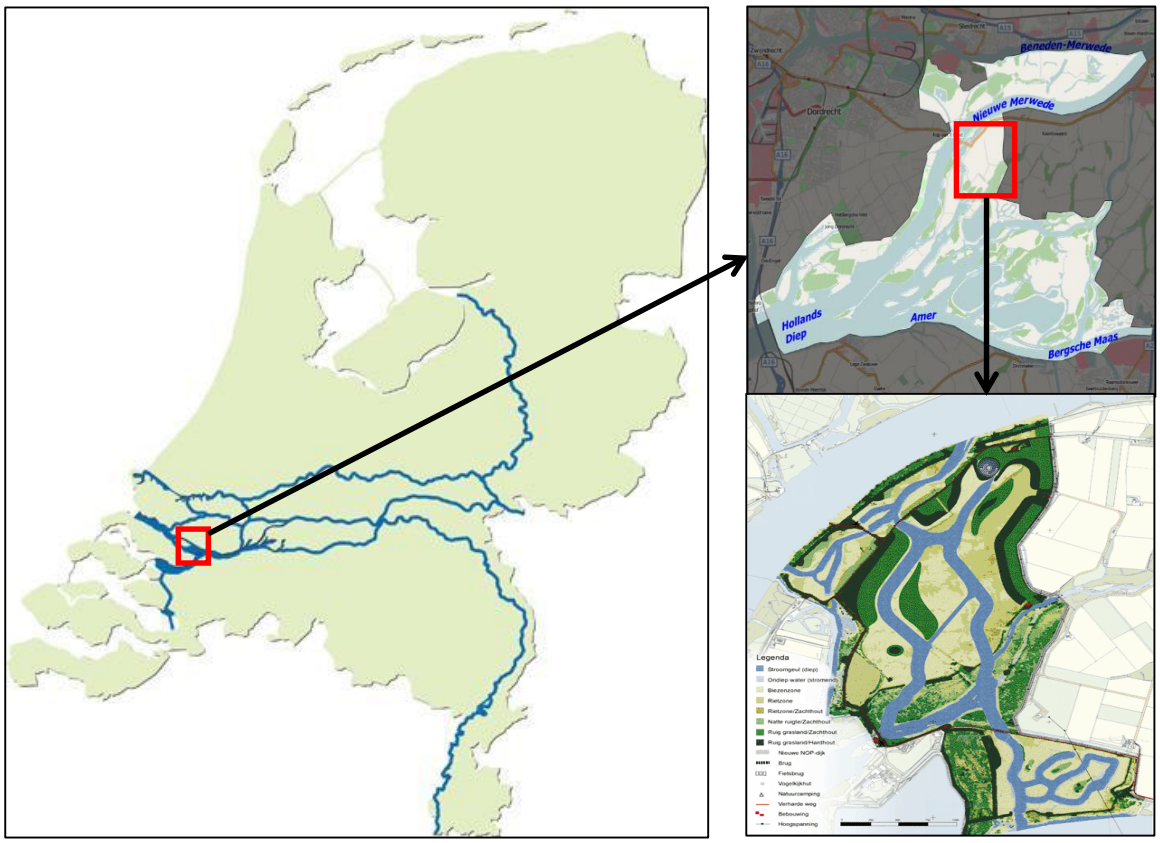

Figure 1. Map of the Netherlands (right), map of the Biesbosch with most important water bodies Nieuwe Merwede, Hollands Diep, Amer and Bergsche Maas (upper left) and vision map of the study area, kleine Noordwaard.

Likewise, the main goal of this research is to determine the composition and origin of the sediment which settled in 'kleine Noordwaard' after reopening the connection to the river 'Nieuwe Merwede'. The source of the freshly deposited sediment is assumed to be both river and polder originated sediment. The river originated sediment is expected to be more polluted in contrast to the reworked polder originated sediment. With this difference in composition it can be calculated whether the sediment is originated from the river or reworked polder sediment within the area. The spatial distribution of different sediment sources gives insight into the morphological pattern within the study area. As for the water and sediment quality, it is crucial to know the spatial position of the contaminated sediment which can become a secondary contamination source if these sediments get reworked. This would have a negative impact on the ecological development of the area.

To get this information, the determination of the origin of the sediment is necessary. This is achieved by examining the composition of 200 sediment samples collected by using different sampling methods. By utilizing the aforementioned fingerprinting techniques for radio-metric and man-induced, the concentration of various elements in the sediment samples will be determined. Considering the variations in composition the different sources will be distinguished and their contribution to the sediment calculated.

2 Study area

First, a brief discussion of the history of the study area. The 'Biesbosch' is an inland delta within the Rhine-Meuse delta in the southwest of the Netherlands (Figure 3). This former estuary of the Rhine and Meuse was drained for agriculture in the Middle Ages (Noordwaard, 2007). A large inland lake was formed by Elisabeth's flood in 1421 AD which has resulted in an inland delta. After the flood the area silted up with Rhine and Meuse sediments from the north east and then the highest parts were embanked for agriculture ((Kleinhans, Weerts, & Cohen, 2010); (Zonneveld, 1960)). The embankment of the study area was accomplished in several steps. Around 1850 the first embankments were built, enabling more agricultural activities in the area. Between 1861 and 1874 the 'Nieuwe Merwede' canal was dug to drain the water from the 'Boven Merwede', a branch of the Rhine, faster (Rijkwaterstaat, 2015). This took place north of the study area and resulted in the relocation of the embankments around the area, causing the water of the 'Nieuwe Merwede' to partially flow through the study area. Afterwards, over the whole nineteenth century, the area was mostly embanked and used for agriculture (Figure 2). Around 1980, the connections from the 'kleine Noordwaard' to the 'Nieuwe Merwede' including the tidal creek 'gat van Leinoorden' were closed off and only the connections to the 'Hollands Diep' and 'Amer - Bergsche Maas' remained (Noordwaard, 2007).

In the second half of the nineteenth century a sequence of dike constructions were built to protect the Dutch coast against the sea. Part of this plan was the building of the 'Haringvliet' barrier in 1970 which closed off the main connection between the 'Biesbosch' and the North Sea. This resulted in a decrease in tidal range from 1 meter to 0.3 - 0.4 meter (de Boois, 1982). This resulted in the depletion of marshland, less sediment supply, the silting up of the smaller creeks due to the erosion of natural banks and increased rates of soil subsidence (de Boois, 1982).

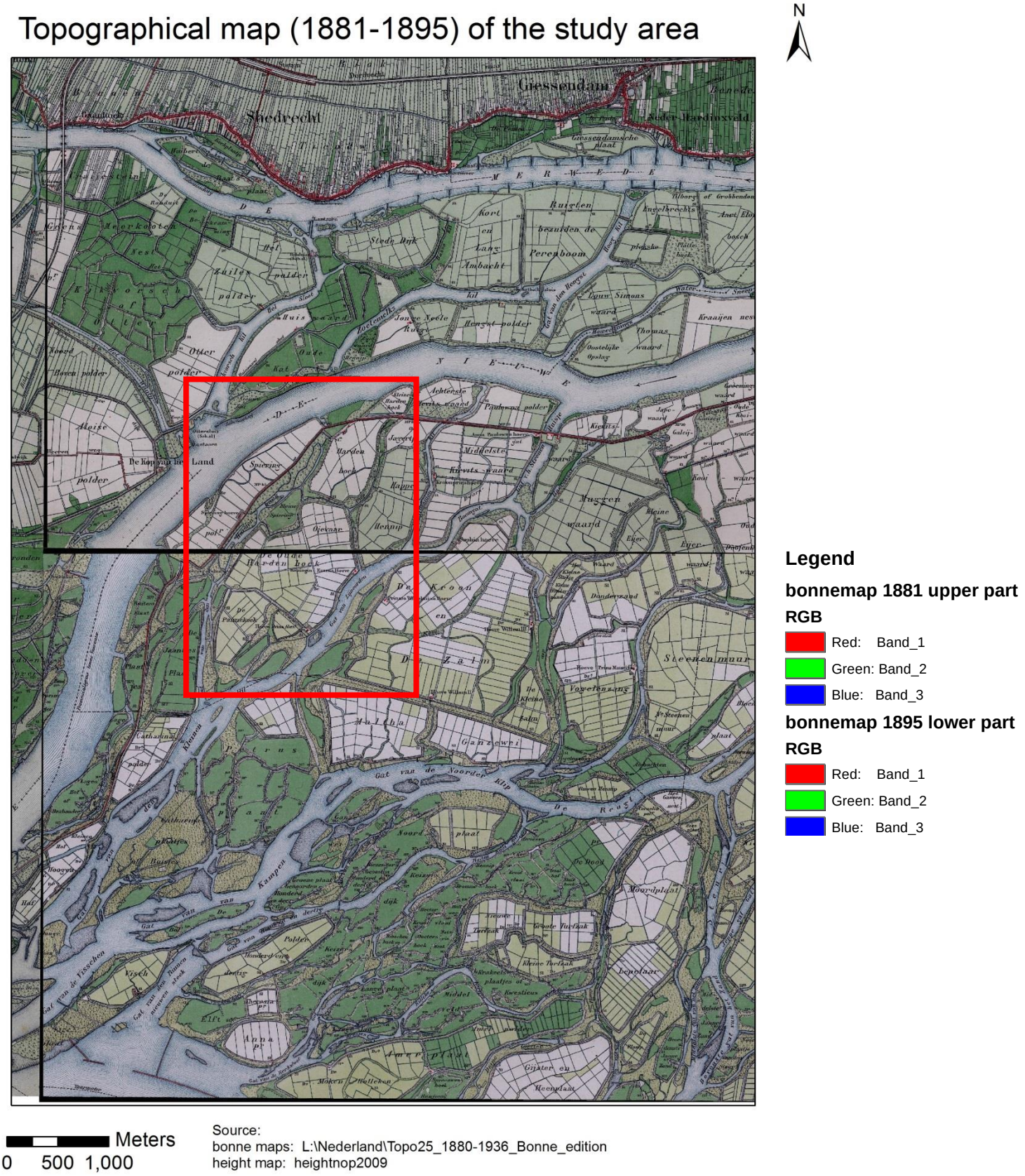

Figure 2. Historical topographical map of the study area from 1881-1895. The red square indicated the location of the study area. White are agricultural areas, light green are pastures, dark green are woodlands, blue is water.

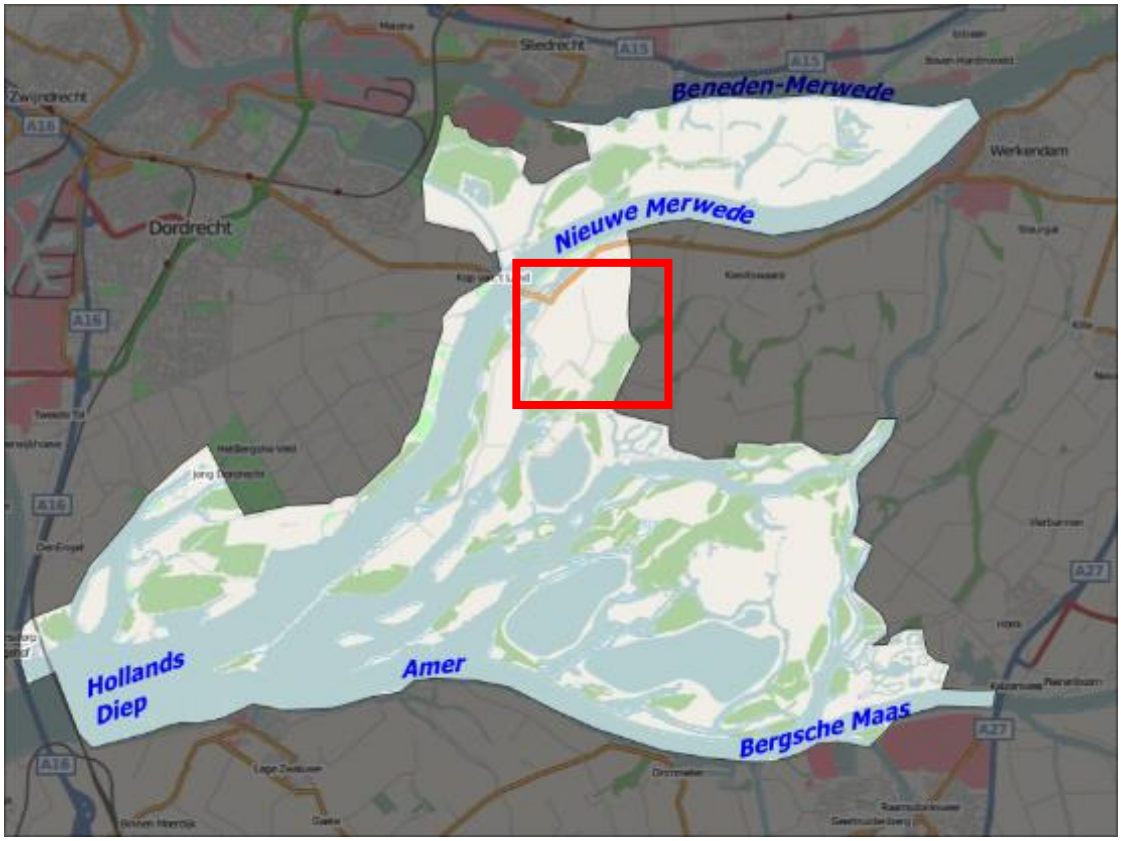

Figure 3. Map of the Biesbosch with most important water bodies Nieuwe Merwede, Hollands Diep, Amer and Bergsche Maas.

Furthermore, a look at the history of the contamination with heavy metals of the rivers in the Netherlands. The deposition of heavy metals into rivers started from the end of the nineteenth century. Due to industrial waste dumping, the heavy metal concentrations in the river Rhine increased during the twentieth century. There were two peak periods with maximal pollution during the 1930s and the 1960s when the cupper, led and zinc concentrations were about 6 to 10 times as high as the background values (Middelkoop, 2000) (Figure 4). From 1970 onwards the zinc concentration has been declining to approximately 400 mg/kg in the Rhine in 2013 (Figure 5). The river Meuse shows a similar trend as the Rhine in the twentieth century but is even more polluted ((Middelkoop, 2000); (van der Perk, 2012)). As a result, the 'Biesbosch' is noted as an area with highly contaminated sediments in the evaluation policy document on water management (Anonymous, 1994).

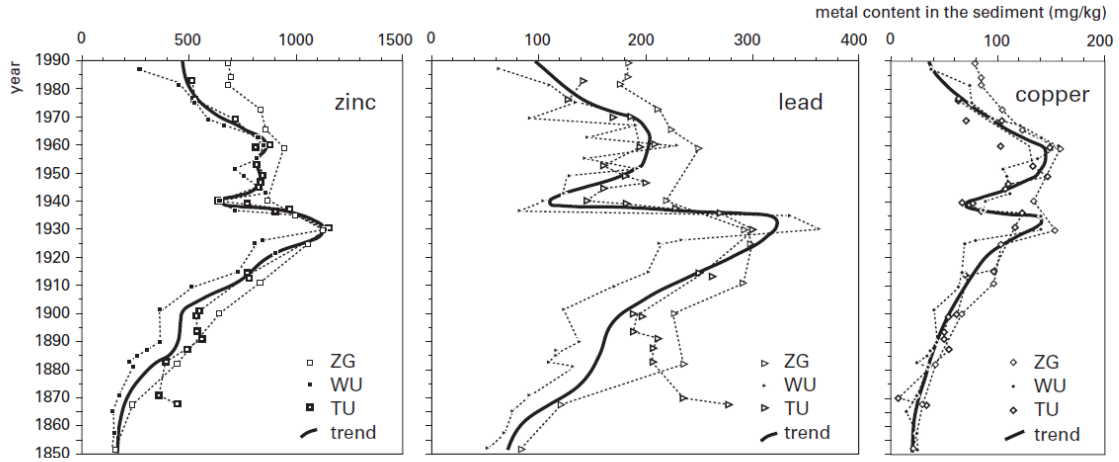

Figure 4. Trend in the copper, lead and zinc concentration of sediment of the lower Rhine over the past 150 years. From Middelkoop, 2000.

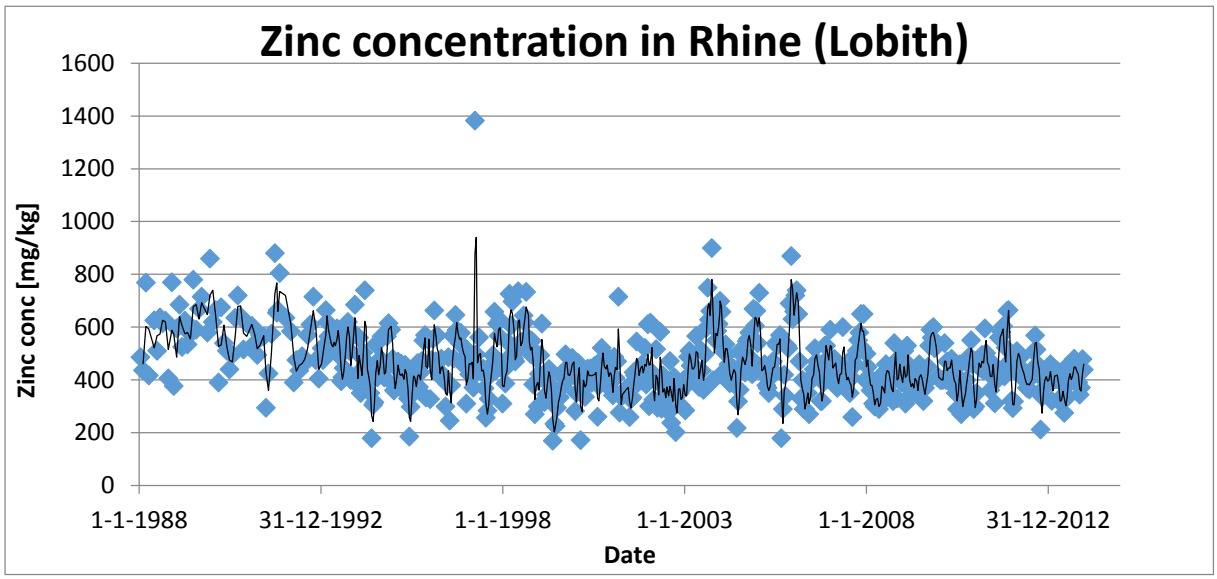

Figure 5. Zinc concentration of the Rhine at Lobith from 1988-2012.

Next to the history of the area and the contamination history of the rivers, the destination plans of the government are important to take into account. In 1990 the 'kleine Noordwaard' was elected to be a nature development region within the nature development plan of the executive agency of the Dutch Ministry of Agriculture, Nature and Nutrition. Later, this destination plan evolved and made the area both nature development region and water management region in the project Room for the River from Rijkswaterstaat, executive agency of the Dutch Ministry of Transport, Public Works and Water Management in 2000 (mRO, 2015). In accordance with this plan, in 2008 the protective embankments were cut through locally causing river water to continuously flow though the previously cultivated 'kleine Noordwaard'. Before the embankment was removed, the former channel pattern and some higher parts were reconstructed using man-made sediment and named rough grassland, hard and soft wood '*ruig grassland, hard en zacht hout*' (Figure 6). To comply with the plan, in the future more embankments in the surrounding areas will be lowered to allow the river to overflow in cases of high water levels. This opening to the 'kleine Noordwaard' allows the river to flow and sedimentate in a twice as large accommodation area. Also, the increased accommodation space will lead to reduced water levels of 30 cm at Gorinchem (Noordwaard, 2007). In the development plan, the predicted climate changes are also accounted for in terms of: increased sea level rise, increased tidal range, increased flood water levels, increased groundwater levels and higher river discharges. To account for these changes, in the plans of adapting the management of the Haringvliet barrier sluices to a more open construction, an increase in tidal range up to 1.0 m is allowed for in the destinations plans.

Figure 6. Vision map of the kleine Noordwaard.

Besides the nature development and increased safety against flooding, this project was also supposed to add value to recreational possibilities in terms of the spatial quality of the study area. So in reality, the study area has been transformed from an agricultural area into a nature development, water management and recreational area as a result of the destination plan.

3 Methods

3.1 Sample collection

The samples were collected in four separate periods, 13th-18th July, 8th -12th September, 6th-10th October and 20th-24th October of 2014. In Figure 7 is shown which sediments were taken in which weeks. In appendix B the larger version of figure 7 is shown. During these weeks several kind of samples were obtained: suspended sediment in jars, containers and grass mats and freshly deposited sediments in plastic bags (Table 1). Freshly deposited sediment thickness observations were done over several transects.

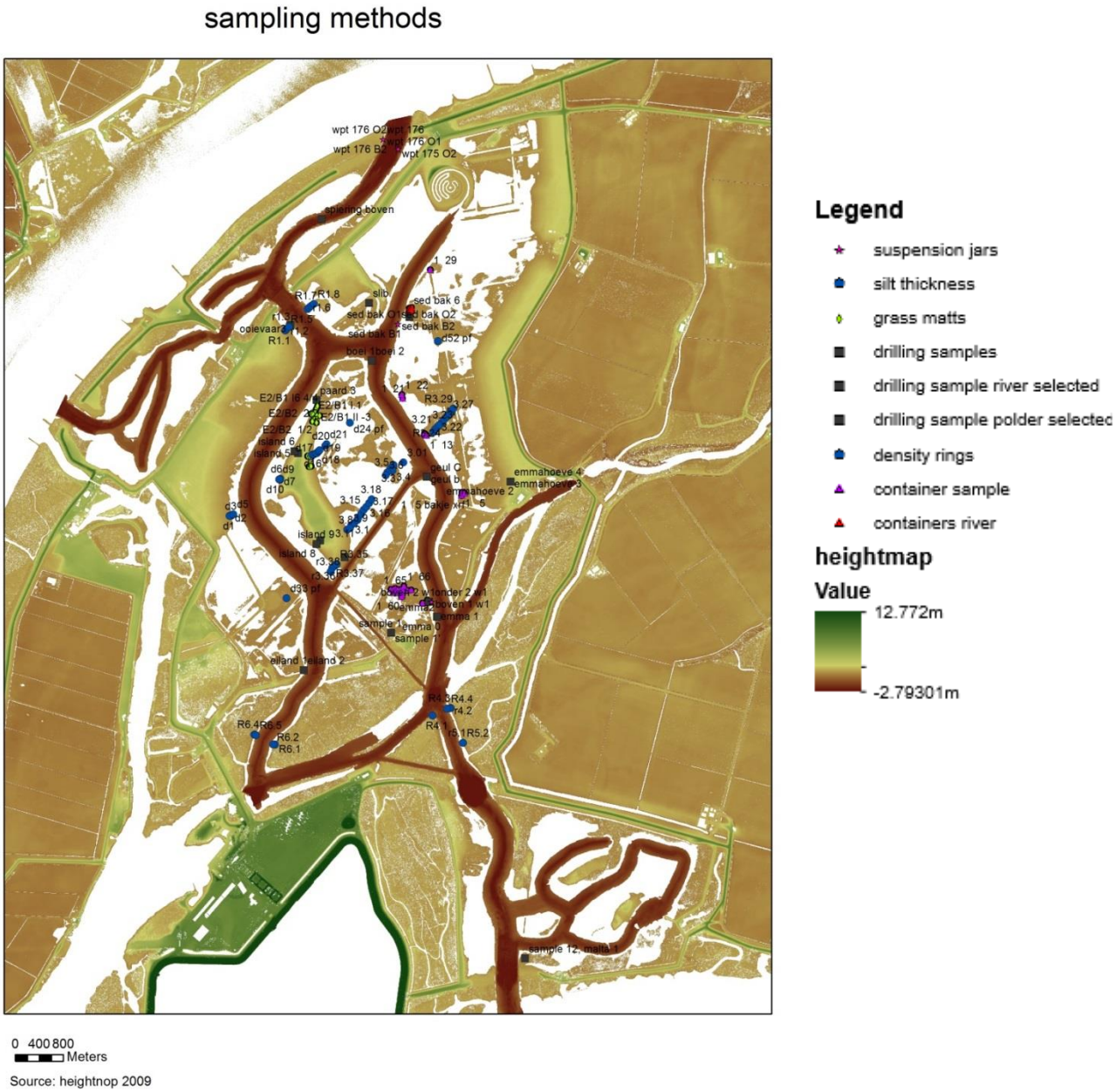

Figure 7. The different sampling methods projected on a height map of the study area. Week 1 in purple, week 2 in red, week 3 in blue and week 4 in black.

3.1.1 Suspended sediment

To determine the composition of the suspended sediment in the water column, jars with a diameter of 7 cm and a height of 10 cm, were placed in the channel at two heights on 5 different locations to trap suspended sediment from the water column. The constructions were placed at the margin of the channel. Because of the depth in the middle of the channel was too deep for placing of the construction into the bottom. In Figure 7 the location of the channel jars is shown.

The suspended sediment settling on the soil was collected to determine the sediment rate and the composition of the freshly deposited sediment. Plastic containers were placed on 7 locations around low water on the ground just above the waterline to trap newly deposited sediment. Seven arrays of plastic containers were placed and secured to the ground with pins. Each array had a row perpendicular to the water line and a row parallel to the waterline with approximately 10m between each container (Figure 7). Each container had a size of 18.5 cm x 11.5 cm x 5 cm. Some containers were higher with a height of 8 cm.

In addition to the plastic containers 54 grass mats were placed to trap sediment. The mats had a size of 50 cm x 50 cm x 15 cm. Some mats were short haired and had a height of 5 cm. The mats were placed in 5 arrays on the island at high water level and higher, with approximately 5 meters between each matt (Figure 7).

This makes a total of 126 sediment traps, containers and mats, which were used to determine the composition of suspended sediment.

3.1.2 Freshly deposited sediment

Auger samples were collected to determine the chemical composition of the top soil or a specific lithology in the soil. The samples were taken with a soil auger on land or a tube corer if the location was in the water. Totally 63 samples were taken shown in Figure 7.

3.1.3 Freshly deposited sediment thickness

The thickness of the freshly deposited sediment was measured to estimate of the amount of freshly deposited sediment in the area. The sediment thickness was recorded at an interval of approximately 50 m along seven transects, a total of 64 samples (Figure 7). The distinction between the freshly deposited sediment and the layer underneath was defined by the compaction of the sediment. The thickness of the freshly deposited sediment was measured with a ruler and at was collected at several locations for heavy metal composition determination.

3.1.4 Density

Density samples were collected to determine the density of the freshly deposited sediment and clay. This is used to determine the fluxes in the study area. The samples were taken using a hollow tube and the thickness of the layers measured. The volume and weight of each layer was determined to calculate a density. For the clay density, stainless steel rings of sample were taken to determine the density. The density rings taken to determine the clay density were used for composition determination of the former polder sediments.

Table 1. Sampling methods used for data analyses (composition sample), reference for polder originated sediment (polder selected) and river originated sediment (river selected).

	Composition samples	polder selected	river selected	total
Suspended sediment containers	38	-	14	52
Suspended sediment jars		-	20	20
Suspended sediment grass mats	54	-	-	54
drilling samples	44	18	1	63
density rings		14		14
Freshly deposited sediment thickness samples	64	-	-	64
total	**200**	**32**	**35**	**267**

The containers and jars were closed, the grass mats were put in garbage bags and the other samples were put in plastic zip bags for transportation and storage. Between sampling and processing the samples were placed in cool bag or refrigerator.

3.2 Laboratory methods

3.2.1 Chemical fingerprinting

First, all the collected samples were transferred to a beaker using distilled water if necessary. Secondly, the samples were dried at 70˚C in an oven, homogenized and put in cups with a polypropylene foil at the bottom.

The samples were measured by the hand held x-ray fluorescence spectrometer (XL3t-46087). All samples were measured with the bulk standard soil method without helium and for at least 30 seconds at main modus, 15 seconds at high modus and 5 sec at low modus (Figure 8). Longer measuring times only produce marginally higher results for Mg, Al and Si (Smeth, 2011). The use of helium was not needed because of the atomic number of the elements is mostly above 20 (Smeth, 2011). The measurement time was optimized using multiple measurements of the same sample. To check the measuring device twenty-eight samples were measured three times and one sample was measured during the whole measuring period. For the ratio calculations the average of the all measurements of 1 sample was taken.

The measured elements were iron (Fe), cupper (Cu), led (Pb), titanium (Ti), rubidium (Rb), zirconium (Zr), manganese (Mn), sulphur (S), strontium (Sr), arsenic (As), vanadium (V), calcium (Ca), potassium (K), nickel (Ni), zinc (Zn), selenium (Se), molybdenum (Mo), tungsten (W), gold (Au), mercury (Hg), thorium (Th), uranium (U), scandium (Sc), chromium (Cr), silver (Ag), cadmium (Cd), Tin (Sn), antimony(Sb), barium (Ba), tellurium (Te) and cerium (Ce), see appendix C.

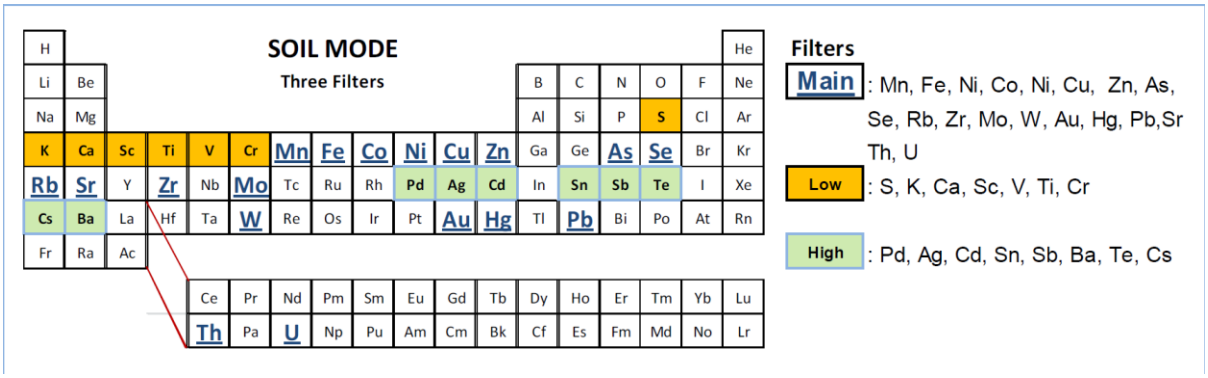

Figure 8. Mode of the hand held x-ray fluorescence spectrometer, presenting the measured elements for each modus.

3.2.2 Radiometric fingerprinting

To determine the relative age of the sediment the total activity concentration of the total sample for each radionuclide is measured. The samples were prepared in three steps. Firstly the samples were dried at 70˚C in the oven and homogenized. Secondly, the samples were weighted and transferred to and evenly distributed and compacted (using a glass tamping rod) in 6 cm Petri dishes. Thirdly, the samples are weighted again and sealed into 50um thick polyethylene bags and stored for at least 2 weeks before measurement. The amount of disintegrates per second per kilogram were measured by a gamma-ray spectrometer. The detection model is BE3830, Canberra BeGe, broad energy Germanium detector with an active diameter of 71 mm, active area of 3800mm² and a thickness of 31 mm. Sample counts, background corrected, were expressed as Bq/kg dry sediment.

$$\frac{\left(\frac{c_S}{t}\right) - cph_b}{m} * factor = \frac{Bq}{kg} \qquad \text{(eq 1)}$$

Where c_s is amount of disintegrates of the sample, t is measuring time in hours, cph_b is the blanco counts per hour which is also known as noise or background values of the measuring machine, m is the mass in gr and factor is the factor to compute cph per gram to Becquerel per kilogram (van Aken, 2013). Background values are estimated by counting sealed empty dishes at different collection times over time. The used detector was calibrated by cross-reference measurements on calibrated detectors in use at 2 different institutes in the Netherlands, One at WGMLA-Radiochemie, Rijkswaterstaat Waterdienst in Lelystad and the other at NIOZ in Den Oever, Texel (van Aken, 2013).

The measured elements are ^{137}Cs and ^{210}Pb, ^{214}Pb, ^{214}Bi and ^{40}K. ^{137}Cs and ^{210}Pb are independent of geology and soil (Motha, Wallbrinka, Hairsinea, & Grayson, 2004). ^{137}Cs is an artificial radionuclide, which has been released into the atmosphere during atmospheric nuclear detonations of the twentieth century with minor contributions from the Chernobyl accident in 1986 (Steinhauser, Merz, Hainz, & Sterba, 2013). The atmospheric nuclear testing reached a climax in 1963 which resulted in the highest peak of ^{137}Cs (Bierman, et al., 1998). The last worldwide release of ^{137}Cs was due to the nuclear disaster with Fukushima Dai-ichi in 2011 (Masson, et al., 2011) . ^{40}K is a type of naturally occurring radionuclide in soils which is expected to be constant in the soil (Kumar, Kumar, Singh, & Singh, 2003).

^{214}Pb and ^{214}Bi are indicators naturally ionization of the atmosphere and thus constant at small spatial scale (Beck, 1974). ^{210}Pb is one of the decay products of ^{238}U decay (see Figure 9). The total ^{210}Pb consist of supported and unsupported ^{210}Pb. A fraction of formed ^{222}Rn diffuses into the atmosphere where it decays into ^{210}Pb. This ^{210}Pb falls out to earth's surface, where is determined to be unsupported ^{210}Pb. It is called unsupported because ^{210}Pb is more abundant than its grandparent ^{226}Ra (Bierman, et al., 1998). Supported Pb-210 is produced by the direct decay of Rn-222 in soil. Supported concentration of ^{210}Pb can be determined by measuring the activity of parent isotopes, such as ^{214}Pb (Bierman, et al., 1998). So ^{210}Pb is larger than ^{214}Pb and ^{214}Bi the sediment of the sample consist of an influx of sediment or the sediment younger than 150 years (van Aken, 2013).

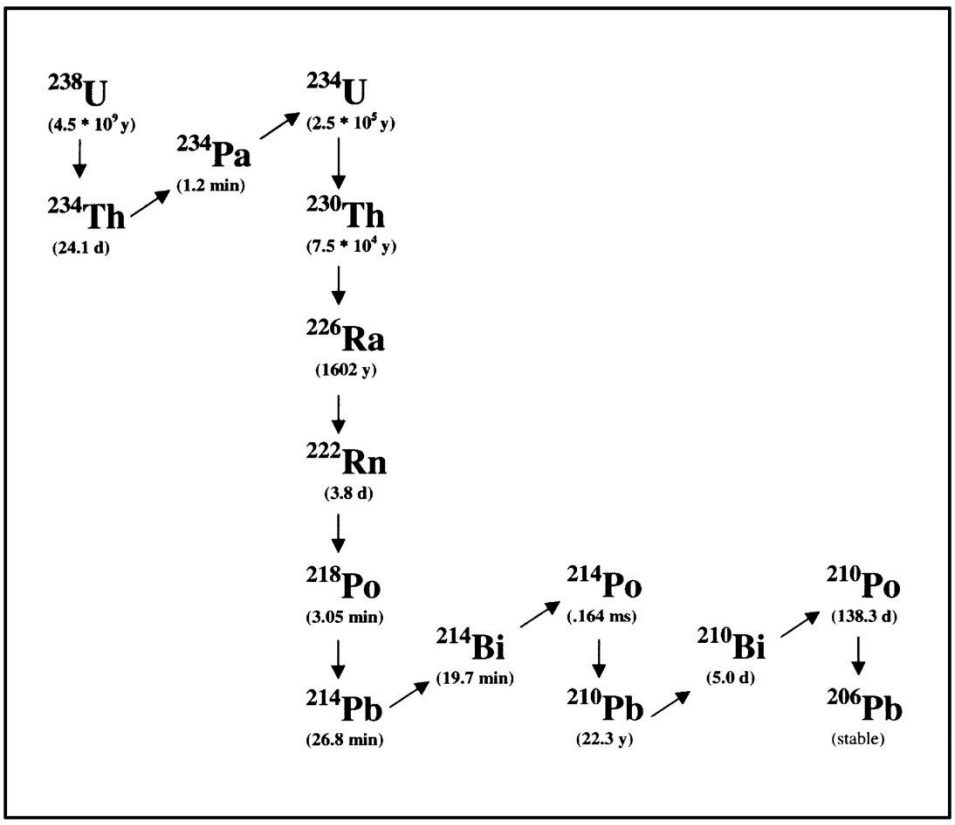

Figure 9. Decay chain of uranium-137 with half life of each daughter.

3.3 Data processing

From the 31 elements measured by the xrf, zinc was selected as indicator for the river input. The metal concentrations in the soil can be considered as a measure of the degree of pollution of the river in the upstream basin (Middelkoop, 1997). Zinc was chosen as an indicator for the river input because of its most distinctness in concentration of polder sediment and river originated sediment in this dataset compared to the other heavy metals such as iron, led, cupper and cadmium. Most elements depend on grain size (Forstner & Salomons, 1980). Rubidium was chosen as indicator for the grain size. Because it positively correlates with illite, Al_2O_3 and K_2O, rubidium is therefore generally abundant in clay and siltstones. Thus, the amount of rubidium may consequently be used a measure of amount of fine-grained, siliclastic material present when comparing sediments from the same provenance (Dypvik & Harris, 2001). With these two elements calculations were conducted to derive a weighted ratio of the two different sediment sources making up the sample.

From the correlation between rubidium and zinc two trend lines are interpreted as different sediment sources (Figure 11, Figure 10). Both lines increase with increasing rubidium concentration, the lower line is interpreted as the less polluted line which represent the samples originated from the polder soil, called the 'polder trend line'. The upper line is interpreted as sediment originated from the river, called the 'river trend line'. For each trend line, samples were chosen for quantify these trend lines using linear regression: The samples selected for the determination of the polder trend line were 14 density samples and 18 freshly deposited sediment samples. The density samples were taken in the clay layer that was abundant deeper underground. The chosen freshly deposited sediment samples were located on higher grounds and were only inundated with extreme high water. The samples selected to determine the river trend line were the suspended sediment from channel, 1 array of suspended sediment containers with high zinc values and one freshly deposited sediment samples in the 'Spiering polder' which is the connection between the study area and the 'nieuwe Merwede' .
The samples which were not selected for the trend lines the original composition is unknown. It is assumed to be only a combination of the incoming polluted river sediment and the 'old' polder sediment. The original composition is statistically determined using linear regression:

$$Zn_{river} = a * Rb_{river} + b \quad \text{(eq 2)}$$

$$Zn_{polder} = c * Rb_{polder} + d \quad \text{(eq 3)}$$

$$Zn_{mix} = x * Zn_{river} + (1 - x) * Zn_{polder} \quad \text{(eq 4)}$$

Where x is the ratio of the polder and river input, Rb_polder and Rb_river are arrays of concentrations drawn from their respective uniform distributions with an increment of 1 ppm. These distribution were based on the minimum and maximum values of the Rb concentration of the samples. The successive array were of the same length to prevent a bias. Zn_{mix} and Rb_{mix} are the Zinc and Rubidium concentrations in the sediment sample measured by xrf. With this input the contribution of both sources is calculated for each sample in a ratio.

$$x = \frac{Zn_{mix} - b*(Rb_{mix} - Rb_{polder}) - c - d*Rb\_polder}{a + b*Rb_{polder} - c - d*Rb\_polder} \quad \text{(eq 5)}$$

$$x = \frac{(Zn_{mix} - c - d*Rb_{mix})}{(a + b*Rb_{river} - c - d*Rb_{river})} \quad \text{(eq 6)}$$

The calculations were split in two parts, polder and river input, because of the unknown composition of the original polder sediment as well as the original river sediment. In the first calculations Rb_{polder} is implemented (see eq 5, 11) and in the second Rb_{river} (see eq 6, 12). For all these ratios of the sample and the successive input a probability of occurrence is calculated. This was done using a normal probability density population with the mean and standard deviation of the selected polder or river samples and used as a weight for the ratio. The weighted ratio is thus calculated by

$$x_w = \frac{\sum_i^n p_i * x_i}{\sum_i^n p_i} \quad \text{(eq 7)}$$

Where p is the probability of occurrence, x the ratio and x_w the weighted ratio.

The weighted ratio consist of an uncertainty which is caused by two sources. Firstly, the uncertainty of the original sediment composition of both sources. Secondly, the uncertainty of the regression prediction of the zinc concentration of both sources. To determine the uncertainty of the weighted ratio a standard error (SE) is calculated

$$SE = \sqrt[2]{s^2 * (1 + \frac{1}{n} + \frac{(Rb_0 - \overline{Rb})^2}{\sum(Rb_i - \overline{Rb})^2}} \quad \text{(eq 8)}$$

Where Rb_i refers to the samples on which the regression line is based. Rb_0 are the samples of which the ratio will be determined. S^2 is the squared standard deviation of the regression, n is the number of samples (Oude Voshaar, 1994)

This standard error is used as standard deviation for the normal distribution of an error, ε which is included into the calculations. Using a Monte Carlo simulation for the standard error, mc, x_2 is calculated

$$Zn_{polder} = a * Rb_{polder} + b + \varepsilon_{polder} \quad \text{(eq 9)}$$

$$Zn_{river} = c * Rb_{river} + d + \varepsilon_{river} \quad \text{(eq 10)}$$

$$x_2 = \frac{(Zn_{mix} - b*(Rb_{mix} - Rb_{polder}) - c - d*Rb_{polder} - mc_{polder})}{(a + b*Rb_{polder} + mc_{river} - c - d*Rb_{polder} - mc_{polder})} \quad \text{(eq 11)}$$

$$x_2 = \frac{(Zn_{mix} - c - d*Rb_{mix} - mc_{polder})}{(a + b*Rb_{r}iver + mc_{river} - c - d*Rb_{river} - mc_{polder})} \quad \text{(eq 12)}$$

Given is x_2, the ratio of the different sources with the error of the regression included. The variance of the ratio with the error caused by the linear regression analysis (x2) represents the total variance in the mixing ratio and the standard deviation the uncertainty of x2. A percentage of variance of x2 and variance of x1 gives the contribution of the regression variance compared to the total variance.

$$Var = \frac{\sum(x - \bar{x})^2 * p}{\frac{\sum p}{(n-1)}} \quad \text{(eq 13)}$$

$$St\ dev = \sqrt{var} \quad \text{(eq 14)}$$

Where x is the calculated ratio, $\bar{x}$ is the mean of the calculated ratio, p is the probability of occurrence and n is the number of samples. The script of the data processing is given in appendix D.

4 Results

4.1 Suspended sediment

In Table 2 the weight and sedimentation rate of the captured sediment are presented per method and location array. The captured sediment with containers of period 1 has on average lower values than period 2 except for array 5, despite the longer measuring time. The most sedimentation occurred in the south of area, west of the eastern channel and near to the tidal creek 'gat van Leinoorden' (array 5). Also the deposited sediment captured with the container method of week 2 has high sedimentation rates, located in the northeast of the study area, east of the eastern channel. Lower sedimentation rates were observed in the southeast (array 1 and 2) and southwest of the study area (array 6). In comparison with the sediment captured with the containers method, the sediment captured with the jar method have higher values. The captured sediment with the jars in the channel have higher values in the bottom height jars in comparison to the top height jars.

Table 2. Weight of sediment captured by containers and jars methods per array. Given by the mean weight, standard deviation weight, mean sedimentation rate, standard deviation of sedimentation rate and amount of samples.

	mean weight [g]	σ	mean sedimentation rate [g/h]	σ	n
week 1	***24,17***	***17,89***	***0,14***	***0,11***	***29***
deposited sediment containers	**24,17**	**17,85**	**0,14**	**0,11**	**26**
array 1	24,39	13,97	0,14	0,08	4
array 2	23,66	18,84	0,14	0,11	6
array 3	15,35	12,19	0,09	0,07	2
array 4	18,36	0,00	0,11	0,00	1
array 5	47,78	26,81	0,29	0,16	4
array 6	16,51	6,62	0,10	0,04	9
sediment in suspension jars	**24,23**	**22,35**	**0,14**	**0,13**	**3**
Top height	11,39	3,00	0,07	0,02	2
Bottom height	49,92	0,00	0,29	0,00	1
week 2	***20,83***	***4,96***	***0,12***	***0,08***	***17***
deposited sediment containers	**40,89**	**3,71**	**0,83**	**0,08**	**13**
sediment in suspension jars	**42,00**	**4,96**	**0,86**	**0,10**	**4**
Top height	37,73	0,54	0,77	0,01	2
Bottom height	46,28	0,56	0,94	0,01	2

4.2 Density

The samples taken to determine the density of the freshly deposited sediment as well as the clay were not used. Due to difficulties in the field these samples were not taken precise enough to deliver accurate density values.

4.3 Chemical fingerprinting

Three line can be distinguished in the graph where zinc is plotted against rubidium (Figure 11). The first line has low zinc values and represents the relatively less polluted samples. The second line with higher zinc values represent the recent deposited sediment which originated from the polluted river sediment. A third line is visible with even higher zinc values. This could represent older tidal creek sediment from the times the Rhine/Merwede and Meuse was more polluted. Because of the few samples found within this third line with very high zinc values, the samples along this line were not taken into account for further calculations of the mixing ratios. The samples representing the polder and river original sediment form two regression lines (Figure 10).

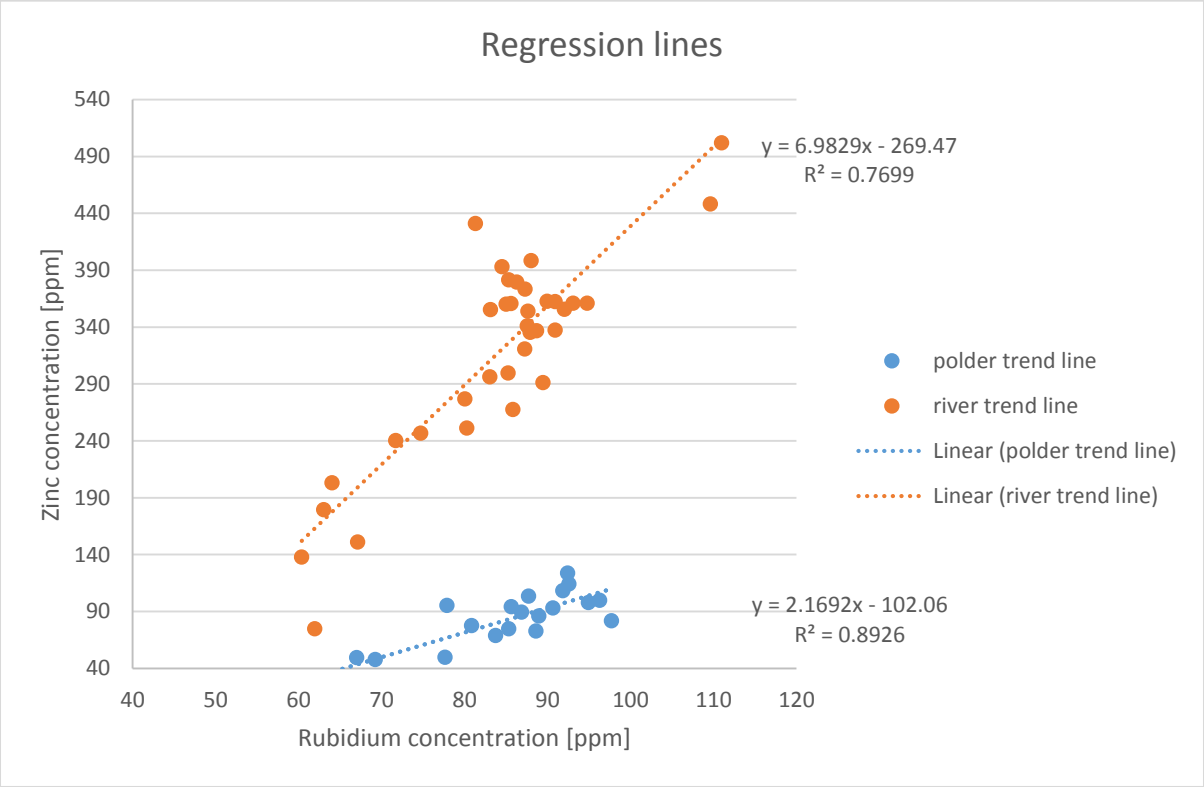

Figure 10. Selected river and polder samples with linear trend lines to determine a, b, c, d.

Three samples were measured several times to control the measuring device, see Table 1. No major differences were found within these measurements.

Table 1. X-ray fluorescence measurements of sample which were measured multiple times.

name	mean Zn [ppm]	St dev Zn [ppm]	mean Rb [ppm]	St dev Rb [ppm]	n
3.25 pf	86	4	89	2	27
geul 3	13	4	57	2	45
sample 1	264	8	80	2	22

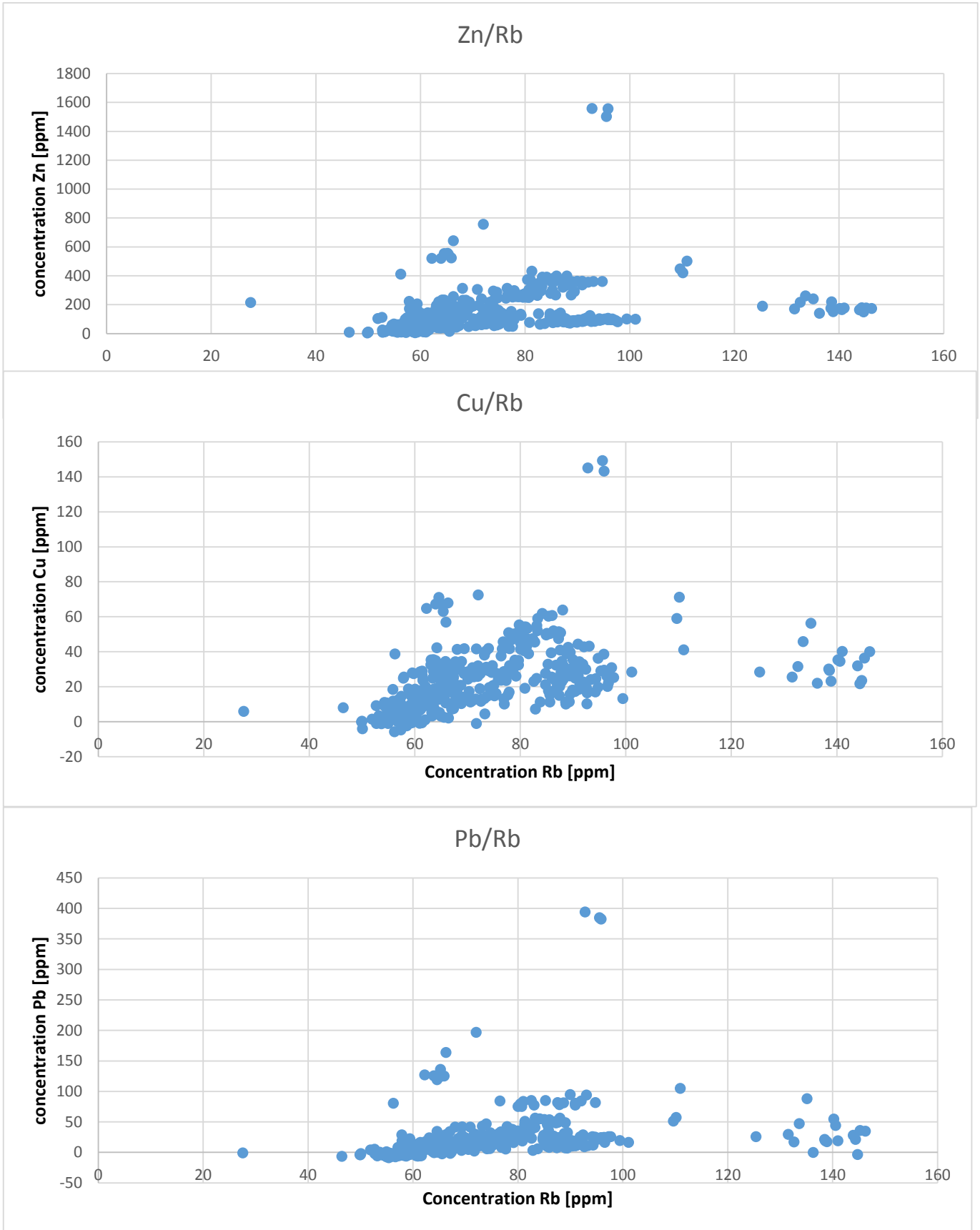

Figure 11. Upper, zinc concentration plotted against rubidium concentration. Middle, cupper concentration plotted against rubidium concentration. Lower, led concentration plotted against rubidium concentration.

4.4 Weighted ratio

The weighted ratio of each array is given in Table 3. The sediment trapped in the grass mats arrays B4 and B1, container array 5 and 6, freshly deposited sediment thickness array 1,4,5,6 and the middle part of array 3 have more input from the river. Notable is the high values for array 6 in the south of the area. More input from the polder is collected by the east and west part of the third array and freshly deposited sediment thickness array 2, containers array 2, grass matts B2 and B3. The weighted ratios for all samples is presented in appendix A. Figure 12 shows the spatial distribution of the weighted ratio which is discussed in detail in following paragraph:

In the north nearby the channel (freshly deposited sediment thickness array 1), the sediment is coming from the river for 59 ± 39% versus 41 ± 39% from the polder. The samples most exterior to the channel have higher weighted ratios.

East of the eastern channel (container array 2) the weighted ratio is 27 ± 9% and the sedimentation rate 0.14 ± 0.11 so mostly sediment originated from the polder has been reworked and redeposited here. More to the south, along the eastern channel (container array 1) the sediment has similar values, a weighted ratio of 32 ± 17% and sedimentation rate 0.14 ± 0.08, indicating a sediment influx originated from the polder.

Between the western and the eastern channel, the sediment captured by containers (array 5 and 6) have relatively high weighted ratio values, although with high coefficient of variation: 167 % and 124 %.

The western side of the study area (freshly deposited sediment thickness array 2) has a 41 ± 41 % river sediment input thus 59 ± 41 polder sediment. However, the west of the western channel and east of island have higher values compared to the east of the western channel, west of the island.

The sediment in the middle of the study area has the highest weighted ratio in the middle part of the array (freshly deposited sediment thickness array 3), indicating a deposition of river originated sediment. The east and west part of the array have lower weighted ratios. The samples located at west side of the island has a higher weighted ratio values than the eastern part.

The weighted ratio of the sediment caught by the grass matts on the island have relatively high coefficient of variation, 95%; 121%; 95%; 90%. The weighted ratio seems to be correlated to the height of the location sediment traps. The high locations have lower ratios then the lower locations. Although the height was not measured accurately, thus this trend is observed by plotting the locations on a height map from 2009 (Figure 12).

South of the island (container array 5, 6), the sediment is on small scale very variable, coefficient of variance of 167 and 124%. The highest and lowest weighted ratio was found here.

Table 3. Weighted ratio per array. Given with samples names, number of samples, mean, standard deviation of the mean x_w and coefficient of variation, cv. Not all samples are mentioned in this table.

Name	samples	n	mean	St dev	cv
Container array 1	1 1 - 1 7	6	0.322	0.168	52%
Container array 2	1 9 - 1 13	5	0.273	0.090	33%
Container array 5	1 35 - 1 44	5	1.892	3.165	167%
Container array 6	1 45 -1 66	18	0.723	0.899	124%
Grass mats B2	E2/B2	8	0.236	0.295	95%
Grass mats B3	E2/B3	12	0.340	0.410	121%
Grass mats B4	E2/B4	7	0.751	0.714	95%
Grass mats B1	E2/B1	27	0.524	0.471	90%
Freshly deposited sediment array 1	1.1-1.8	7	0.587	0.386	66%
Freshly deposited sediment array 2, Transect 1, west of western channel	d1-d5	4	0.415	0.412	99%
Freshly deposited sediment array 2, Transect 2,east of western channel, west of island	d6-d10	4	0.135	0.067	50%
Freshly deposited sediment array 2, Transect 3, east of island	d11-d21	8	0.361	0.217	60%
Freshly deposited sediment array 3, Transect 1, western part	3.35-3.38	4	0.358	0.258	72%
Freshly deposited sediment array 3, Transect 2 middle part	3.08-3.18	11	0.878	0.261	30%
Freshly deposited sediment array 3 Transect 3,middle part near channel	3.01-3.07	6	0.512	0.329	64%
Freshly deposited sediment array 3, Transect 4, eastern part	3.19-3.34	10	0.150	0.112	75%
Freshly deposited sediment array 4	4.1-4.4	4	0.771	0.260	34%
Freshly deposited sediment array 5	5.1-5.2	2	0.846	0.596	70%
Freshly deposited sediment array 6	6.1-6.4	4	1.970	0.582	30%
Drilling samples	island 1,2	2	1.111	0.420	38%

The weighted ratio of each sampling method is given in Table 4. The sediment caught by containers has more input from the river, the grass mats and freshly deposited sediment thickness are both around 50% so both sources seems to have approximately equal input. Notable is the high standard deviation of all of the sampling methods, indicating large differences within one method.

Table 4. Weighted ratio of different sampling methods. Given with amount of samples, mean of weighted ratio and standard deviation of weighted ratio.

	n	mean x_w	St dev x_w
containers	37	0.71	1.21
grass matts	54	0.47	0.49
freshly deposited sediment thickness	64	0.59	0.52
drilling samples	42	0.40	0.57

In total 123 samples received most sediment from polder and 77 samples from river. Giving an average weighted ratio of 43% of the river originated sediment against 57% of polder originated sediment.

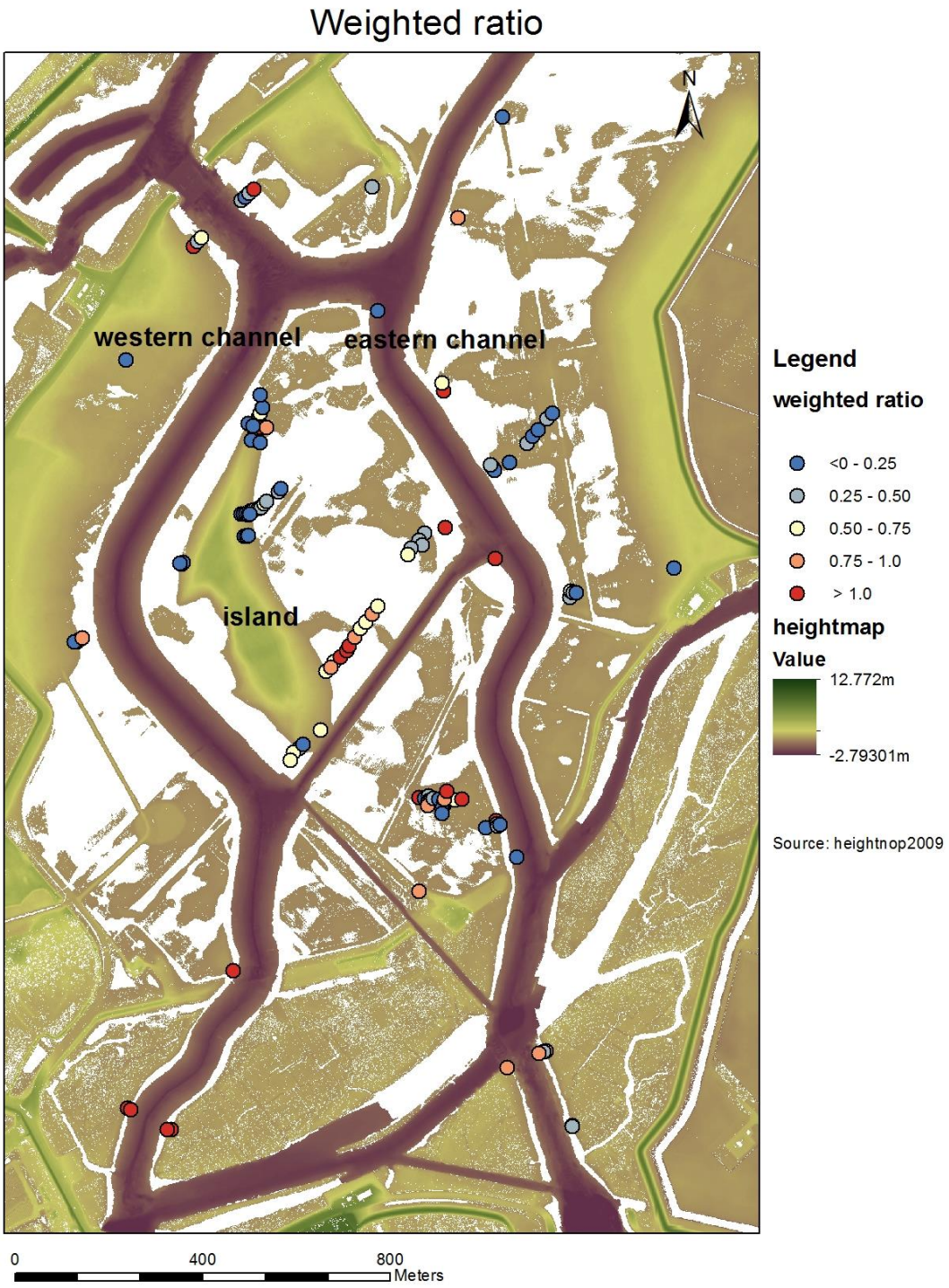

Figure 12. Spatial distribution of the weighted mixing ratio of river sediment versus polder sediment, projected on height map

4.5 Uncertainty estimation

The average variance of the weighted ratio for each sample is 0.0074. In this dataset a linear regression analysis is included to determine the two different sources of sediment. The linear regression analysis adds a residual variance on top of the variance of the data processing. The percentage of the residual variance against variance of data processing is given in Table 5. This indicates that 86 ± 38% of the total variance is caused by the unknown original composition. The other 14± 38% is related to the linear regression analysis.

Table 5. The percentage of the error due to the unknown original composition against the error due to linear regression analysis. Pol is for the polder calculations with the input of the Rb_polder and Riv has Rb_river as input.

	Pol	Riv	total
mean	85	88	86
St dev	25	29	38

4.6 Freshly deposited sediment thickness

The mean freshly deposited sediment thickness for every walked transect is shown in Table 6. The freshly deposited sediment thickness per array and vertical soil profile is given in

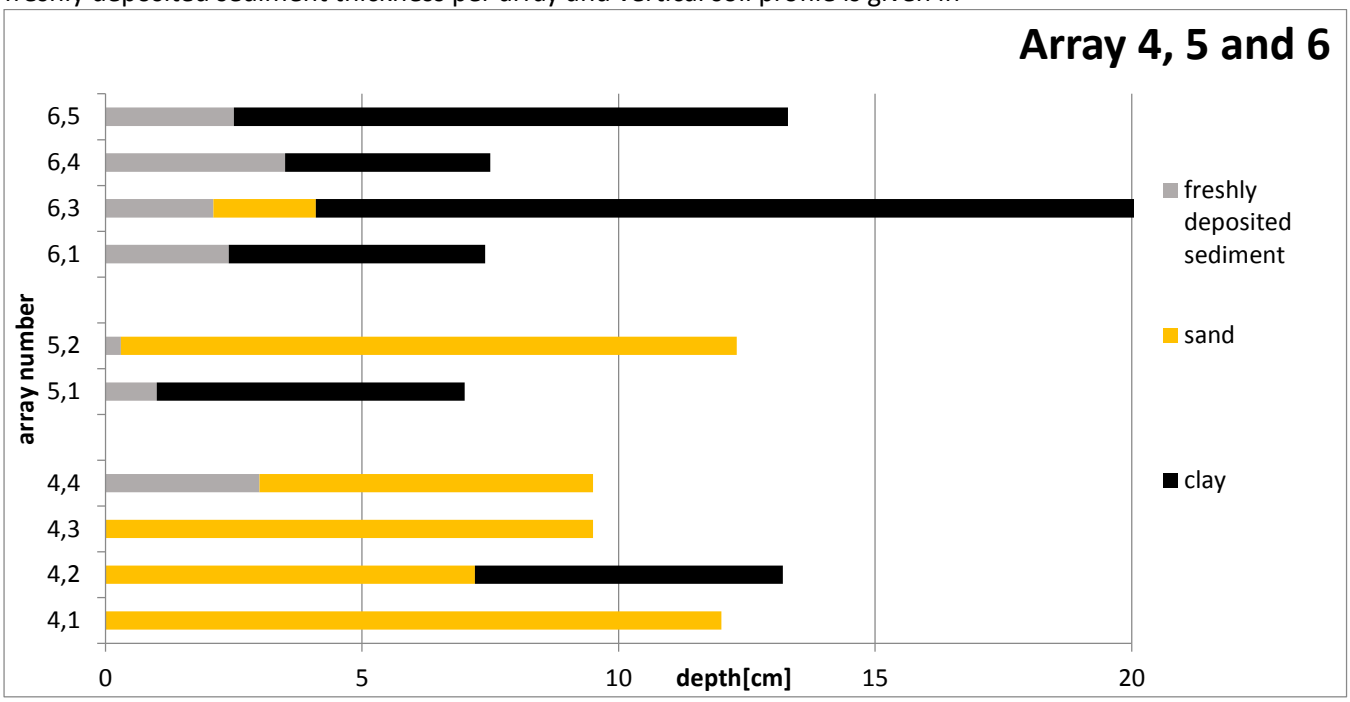

Figure 13. The thickest freshly deposited sediment layer is found in the middle of the study area, south of the island and west of the eastern channel (array 3 transect 4). The whole third array has large freshly deposited sediment thickness values. Other thick freshly deposited sediment layers can be found at the most southwestern corner of the study area (array 6) and located at the north side of the island from west to east (array 2). Specially east of the island (array 2, transect 3). But the overall standard deviation is very large over the area, throughout the area as well as on a small scale (within an array).

The vertical soil profile is mostly sand at the top at the east and west sides of the study area. In the middle part of the area the freshly deposited sediment lies mostly on top, sand beneath it and clay at the bottom, or the top freshly deposited sediment is located directly on the clay. Further south in the study area the freshly deposited sediment on clay as well as the freshly deposited sediment on sand and freshly deposited sediment on sand on clay occurs without notable distribution pattern.

Table 6. Freshly deposited sediment thickness per array. Given with samples names, mean of freshly deposited sediment thickness, standard deviation of mean freshly deposited sediment thickness, coefficient of variation (cv) and number of samples.

freshly deposited sediment thickness	Mean	st dev	cov	N
array 1, north of study area	0.41	0.75	183%	9
array 2, central in study area, north side of island	1.38	2.03	68%	53
transect 1, west of western channel	0.10	3.30	3304%	25
transect 2, east of western channel, west of island	0.81	1.75	215%	8
transect 3, east of island	3.27	1.63	50%	12
transect 4, east of eastern channel	1.33	1.44	108%	8
array 3, central in study area, south side of island	2.26	2.63	116%	65
transect 1, west of western channel	1.75	1.36	78%	8

transect 2, east of western channel, east of island	0.00	0	0%	4
transect 3, west of island	3.34	1.39	241%	11
transect 4, west of eastern channel	4.58	3.71	124%	32
transect 5, east of eastern channel	0.36	0.76	47%	10
array 4, southeastern of study area	0.75	1.50	200%	4
array 5, southeastern of study area	0.65	0.49	76%	2
array 6, southwestern of study area	2.63	0.61	23%	4

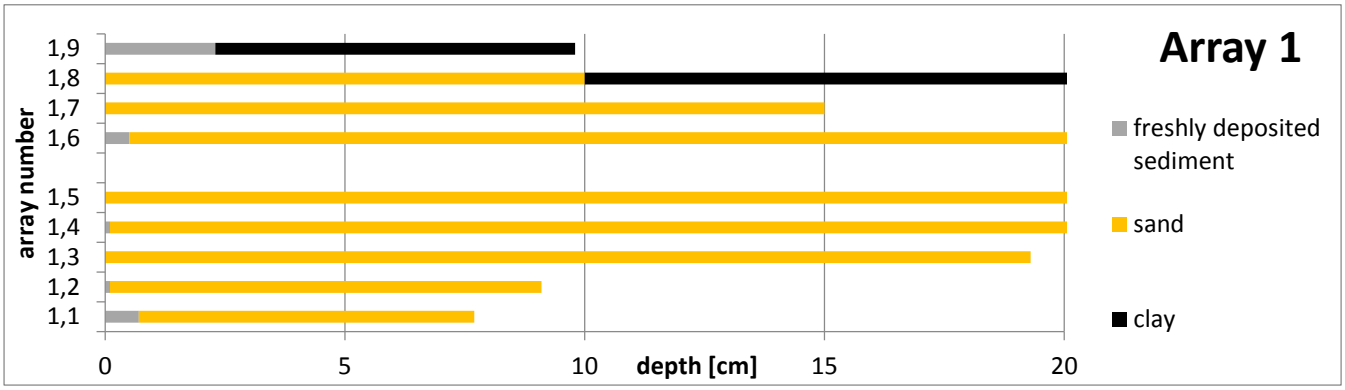

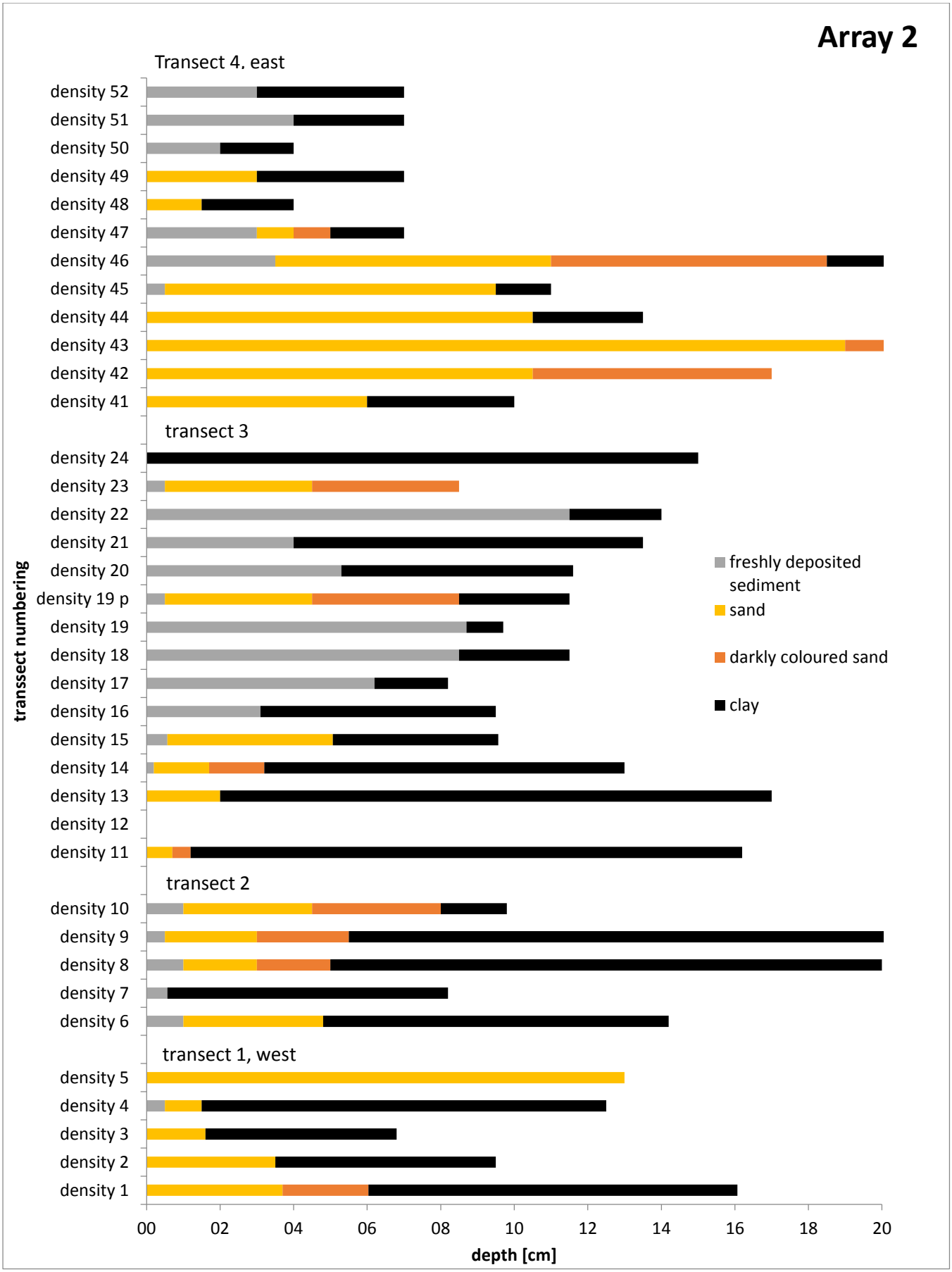
Array 2
Transect 4, east
density 52
density 51
density 50
density 49
density 48
density 47
density 46
density 45
density 44
density 43
density 42
density 41
transect 3
density 24
density 23
density 22
density 21
density 20
density 19 p
density 19
density 18
density 17
density 16
density 15
density 14
density 13
density 12
density 11
transect 2
density 10
density 9
density 8
density 7
density 6
transect 1, west
density 5
density 4
density 3
density 2
density 1
transsect numbering
freshly deposited sediment
sand
darkly coloured sand
clay
00
02
04
06
08
10
12
14
16
18
20
depth [cm]

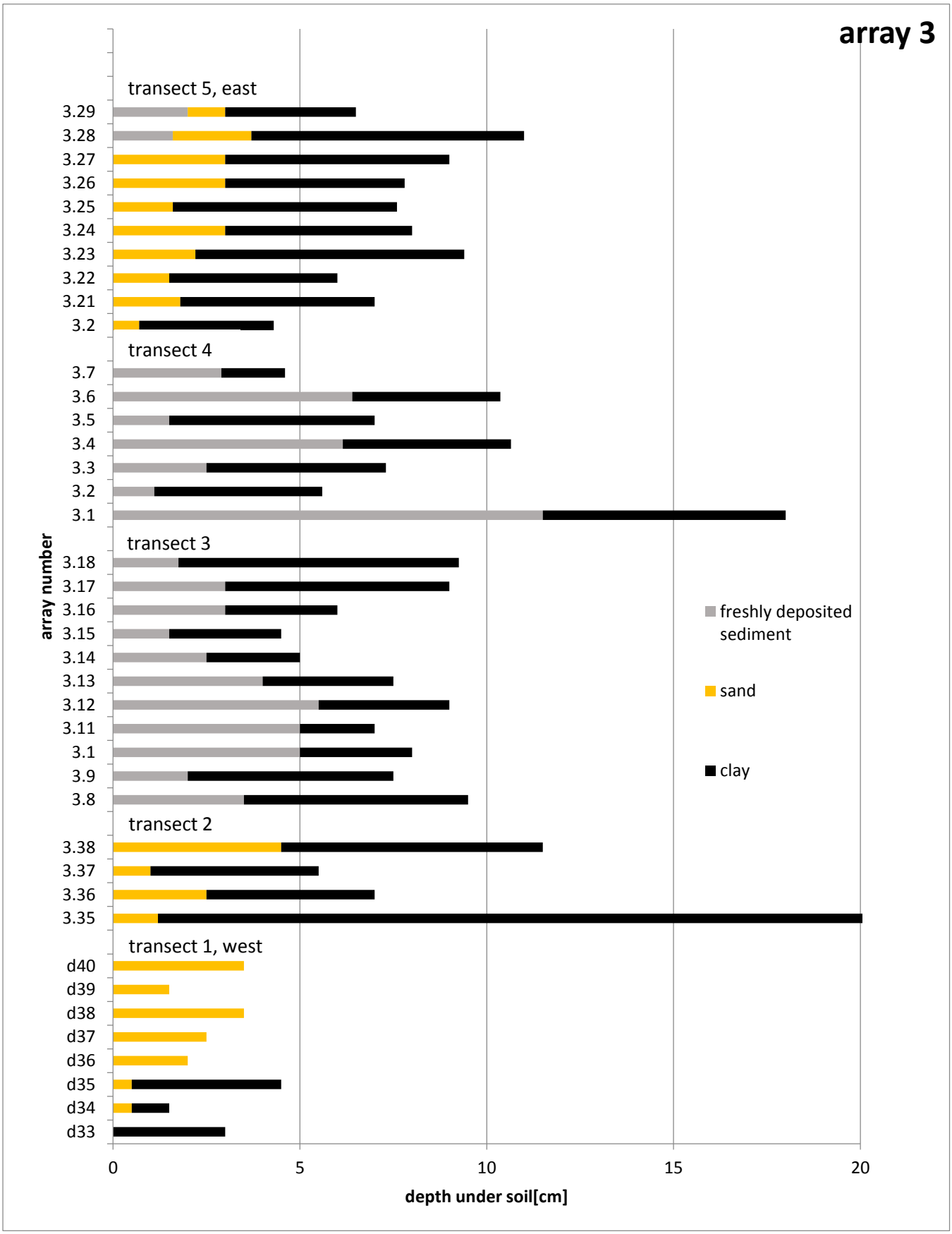
array 3
transect 5, east
3.29
3.28
3.27
3.26
3.25
3.24
3.23
3.22
3.21
3.2
transect 4
3.7
3.6
3.5
3.4
3.3
3.2
3.1
transect 3
3.18
3.17
3.16
3.15
3.14
3.13
3.12
3.11
3.1
3.9
3.8
transect 2
3.38
3.37
3.36
3.35
transect 1, west
d40
d39
d38
d37
d36
d35
d34
d33
array number
freshly deposited sediment
sand
clay
0
5
10
15
20
depth under soil[cm]

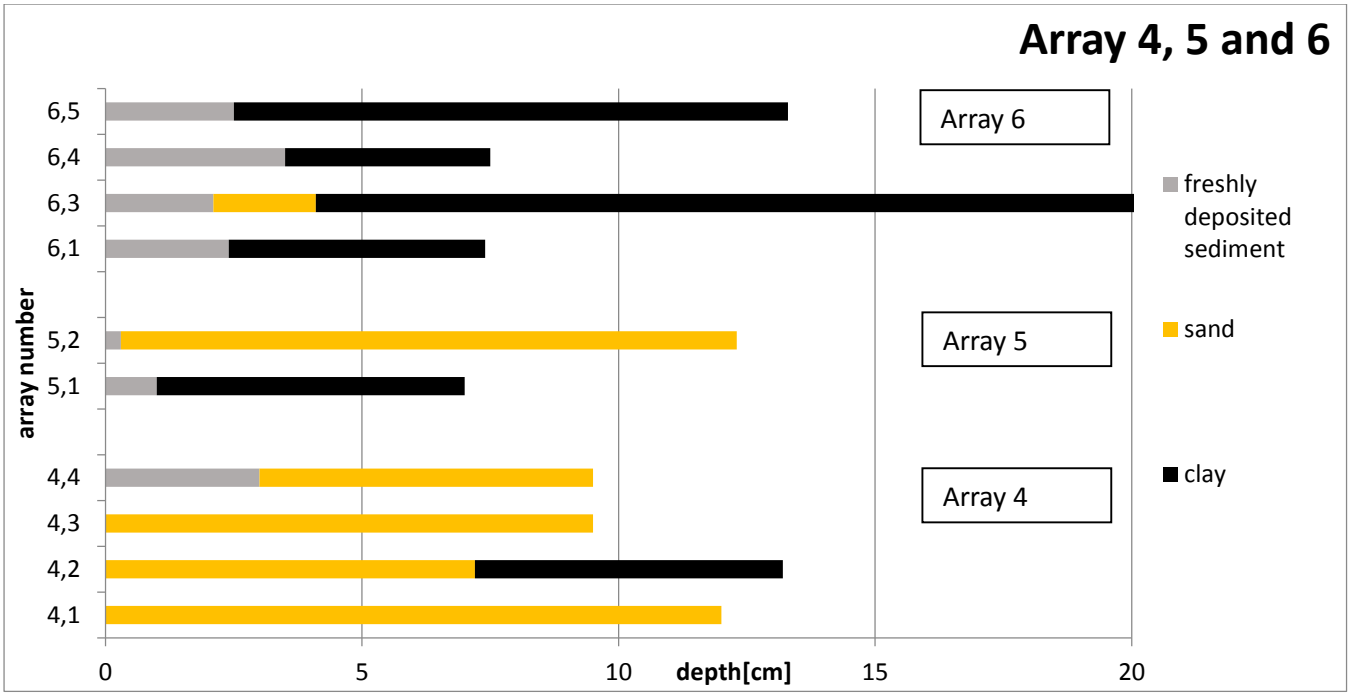

Figure 13. Freshly deposited sediment thickness per array and transect. The flocky top layer which is most freshly deposited sediment is indicated in grey.

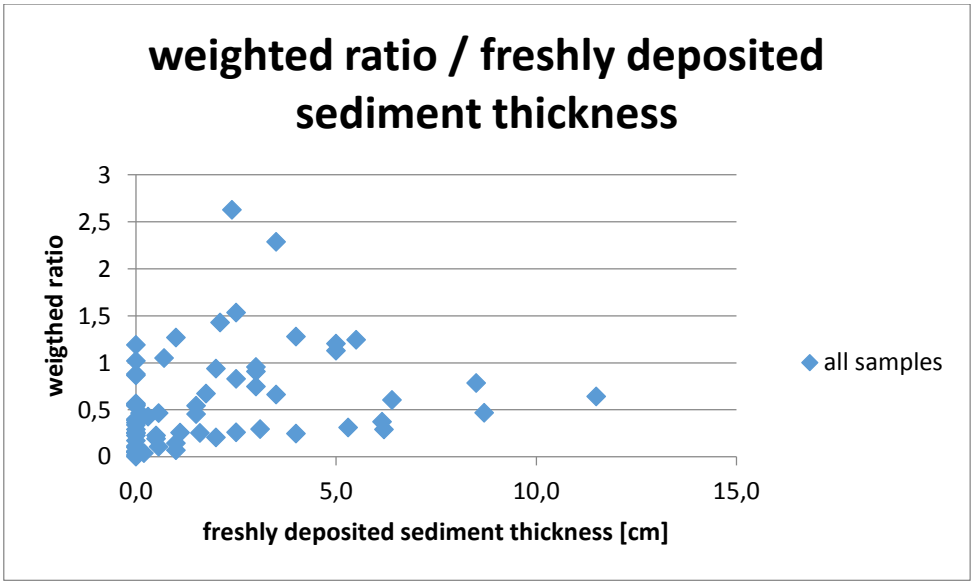

Figure 14. Weighted ratio plotted against freshly deposited sediment thickness for all samples.

Expected is a larger freshly deposited sediment thickness with a larger weighted ratio due to the higher the weighted ratio is the more sediment is coming in. However the sediment supply for the freshly deposited sediment thickness can also be eroded and redistributed sediment from within the area. The relationship between weighted ratio and the freshly deposited sediment thickness is shown in figure 14. With the increasing freshly deposited sediment the minima of the weighted ratio increases.

4.7 Radiometric fingerprinting

The radio-active decay of each element is given in Table 7. The cesium values are lower than the noise of the measuring device and were therefore not used in further analysis. ^{214}Bi, ^{214}Pb are approximately constant in all samples. ^{40}K is constant except for the 'sample 3'. ^{210}Pb has high values at the top samples 'sample 2.1' and 'sample 1'. Lower values of ^{210}Pb are found in samples deeper under the soil. 'Sample 3' seems to be deviating from the other samples. ^{210}Pb is larger than ^{214}Pb and ^{214}Bi in most samples except for the bottom of the 'sample 2 core' and sample 3.

^{210}Pb increases with increasing weighted ratio (Figure 15). The sediment flux positively influences the total ^{210}Pb. The sediment flux is partly represented by the weighted ratio because a high weighted ratio means a higher percentage of river originated sediment and thus a larger flux of incoming sediment. So it is expected that ^{210}Pb values and weighted ratio are depended factors of each other.

Table 7. Radio-active decay of six samples with sample description, mean and standard deviation of the mean. (Some values are below detection limit, <dl)

Name sample	place in core	description sample	^{210} Pb [Bq/kg]	^{214} Pb [Bq/kg]	^{214} Bi [Bq/kg]	^{137} Cs [Bq/kg]	^{40} K [Bq/kg]
Sample 1	Only sample	in old trench	83,64	31,62	39,15	< dl	43,13
Sample 2.1	bottom	Sand	15,17	18,91	22,43	< dl	53,74
Sample 2.2		silt	36,62	29,92	27,74	< dl	61,36
Sample 2.3		sand	46,34	26,81	26,32	<dl	49,81
Sample 2.4	top	sand/silt in suspen-sion	85,17	26,54	35,29	< dl	52,27
Sample 3	top	sand	29,89	33,43	31,00	< dl	5,23
Mean			**49,47**	**27,87**	**30,32**	**-**	**44,26**
St dev			**28,90**	**5,14**	**6,13**	**-**	**20,01**

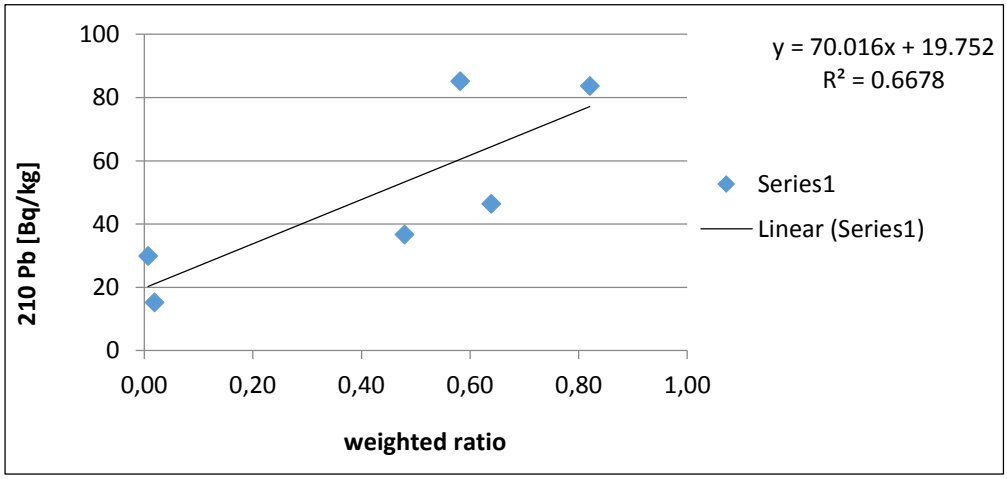

Figure 15. Weighted ratio plotted against radio-active decay of led-210 with a trend line.

5 Discussion

The zinc concentration, normalized for grain size by rubidium, provides a rough estimate of the source of the incoming sediment. This research compares the dataset of the 'kleine Noordwaard' to other datasets in the Netherlands (table 8) ((Middelkoop, 2000) and (Rijkswaterstaat, 2015)). In comparison, the mean, minimum and maximum of this dataset differ from the other datasets. The mean of the sediment in the 'kleine Noordwaard' deviates largely from the measurements of Rijkswaterstaat and Middelkoop. This can be explained by the many samples with sediment that originated from the polder. The majority of the polder originating sediment was deposited before the end of the nineteenth century when human activities in the Rhine catchment increased the metal concentrations in the sediment. The fact remains, sediment from the selected samples, making up the river regression line, still has a slightly lower zinc concentration than the measured sediments have near Lobith, Waal and Meuse. The reason behind this is still unknown and needs more research. The minimum and maximum of the 'kleine Noordwaard' are more extreme in comparison to Lobith, Waal and Meuse. The minimum is due to the polder sediments which are not polluted with the zinc from the river. The maximum is probably due to the older deposits of the river Rhine or Meuse in the south of the area. When these deposits were formed the river Rhine was still more polluted which explains the maximum of this dataset.

Table 8. Zinc concentration of soil and suspended sediment from kleine Noordwaard in comparison to Lobith (Rijkswaterstaat 2015), Waal and Meuse (Middelkoop 2000) in the Netherlands with mean, standard deviation of the mean, minimum and maximum.

	Lobith Jan 1988-Dec 2013 (Rijkswater-staat 2015)	**Lobith Jan 1988-Dec 2013 (Rijkswater-staat 2015)**	**Waal Dec 1993 (Middel-koop 2000)**	**Meuse Dec 1993 (Middel-koop 2000)**	**Kleine Noordwaard Jun-Oct. 2014** ***Total dataset***	**Kleine Noord-waard Jun-Oct. 2014** ***River selected sediments***
zinc content	suspended sediment	Channel sediment	Floodplain soil Rhine	Floodplain soil Meuse	Polder soil	Freshly deposited sedi-ment/suspended sediment
	[mg/kg]	[mg/kg]	[mg/kg]	[mg/kg]	[mg/kg]	[mg/kg]
Mean	460	585	344	684	163	318
St dev	123	281	77	339	170	90
max	1383	962	462	1177	1557	502
Min	170	158	152	94	4	75
N	604	7	41	17	200	35

Also, a weighted ratio lower than 0.5 indicates sedimentation with reworked sediment originated from the polder or no sedimentation at all. A weighted ratio higher than 0.5 indicates sedimentation with sediment originated from the river. From the incoming captured sediment 57 % had the polder as source versus 43 % with river as source.

The extreme high zinc concentration of the freshly deposited sediment thickness array 6, two drilling samples and three sample collected by containers are striking (table 2). In the regression

analysis only two sources were distinguished, polder and river. In the graph of zinc against rubidium a third line became apparent. In the spatial distribution these extreme high values of zinc concentration were all located nearby an old tidal creek, 'gat van Leinoorden' (Figure 16). This old tidal creek could have had two sediment supply sources. Firstly, until 1980 this tidal creek was an open branch of the 'Nieuwe Merwede'. The Rhine was more contaminated with heavy metals, such as zinc, until the 1960s than nowadays. This explains the extreme high zinc concentrations along the tidal creek. Secondly, sediment from the Meuse could have been supplied by tidal currents. The Meuse was more heavily contaminated with zinc than the Rhine, which could be another explanation for the high zinc concentrations ((Middelkoop, 2000) and (van der Perk, 2012)). To further determine the source of the polluted sediment, original Meuse sediment samples should be sampled and besides zinc, at least one other metal should be taken into account in the sediment fingerprinting.

The most southern samples of the study area, along the eastern channel (freshly deposited sediment thickness array 4 and 5) also have a high weighted ratio although lower than in the south of the study area, along the western channel (freshly deposited sediment thickness array 6 and the drilling samples island 1 and 2). Multiple explanations for these locations are possible: all of the deposited sediment is originated from the river or the deposited sediment is a mix of the river sediment from the current 'Nieuwe Merwede' combined with reworked tidal creek deposits. Or the deposited sediment is a mix of reworked polder sediment and reworked tidal creek deposits. More research is needed to determine the exact explanation.

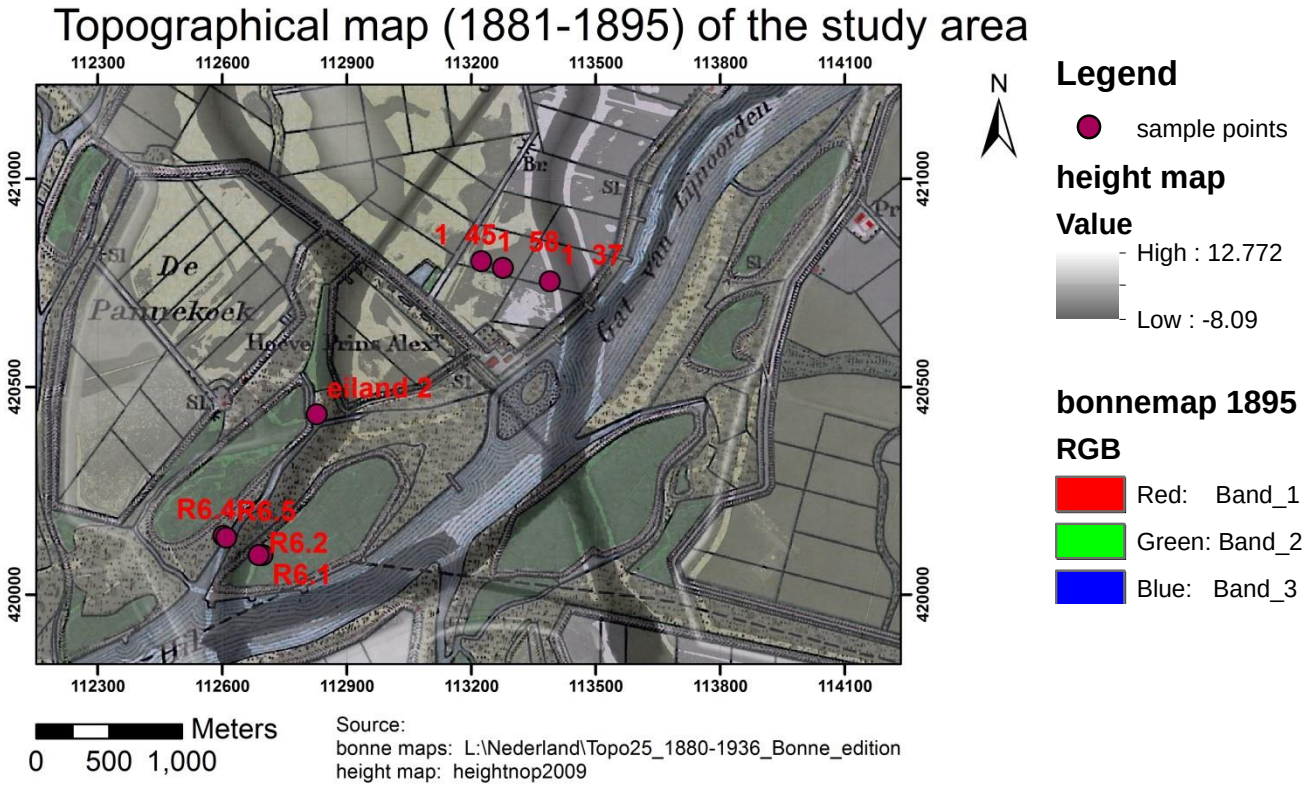

Figure 16. Topographical map of the kleine Noordwaard, 1881-1895, shaded by modern height map. Samples with high weighted ratios are plotted into the map.

Around the island the weighted ratio is slightly larger than the surrounding areas. This is probably due to the human influence on the island. To elevate the island, polder sediment and imported sediment, which contained mainly sand, were used. For unknown reasons this man-made mix of sediment has higher zinc concentrations than the polder originated sediment. The island has erosion scars which indicates reworking of man-made sediment, adding man-made sediment as source for the study area. The sediment from the middle part of freshly deposited sediment thickness array 3 has lower weighted ratios due to reworked polder sediment or man-mixed sediment which has eroded from the island. On the east side of the island, this man-mixed input seems to be less than on the west side. Logically this is because the east side of the island has less erosion scars than the west. The sediment of freshly deposited sediment thickness array 2 at the west side of the island has higher weighted ratio values than the eastern part, due to the erosion of man-made sediment on the island which was deposited at this side of the island.
The weighted ratios mostly increase with larger distance to the channel within an array. This increase in river input is caused by lower water depth which increases sedimentation.

Then there is the statistical error that is caused by the computation for the weighted ratio. The statistical error is low thus the main trends in the area were not affected by the implemented error, caused by the unknown original composition and the regression line, made to quantify the sediment sources.

Furthermore, the second fingerprinting method needs more research. The activity concentration of ^{210}Pb has higher values in the sediment at the top of the soil. At two topsoil samples, ^{210}Pb is larger than ^{214}Pb and ^{214}Bi. This suggests that the sediment of the sample is from an influx of ^{210}Pb rich sediment or that the sediment is younger than 150 years (van Aken, 2013). Due to the low number of samples, however, no conclusions can be drawn by this method.

In this research, the sampling locations are assigned by weighted ratio and sedimentation rate to receive sediment from a certain source (Table 9). Most samples consist of sediment originated from reworked polder sediment mixed with man-made reworked sediment. It should be noted that the location of the samples was not evenly distributed over the area. In Figure 17, the distribution of the four different sediment sources in the study area is shown. In the north and south the river sediment is the most apparent, as it is around the third freshly deposited sediment array in the middle. In the middle of the study area reworked polder sediment is the most discernible as a source and around the island man-made sediment is mostly the source of the sediment. A similar spatial pattern is shown by the freshly deposited sediment thickness. The correlation between freshly deposited sediment and the weighted ratio is low but an increasing trend in freshly deposited sediment with increasing minima of the weighted ratio can be observed (Figure 14). The vertical soil profile indicates a slightly different spatial distribution: mostly sand at the top of the soil at the east and west side of the study area and in the middle of the area the freshly deposited sediment lay on top.

Table 9. Sediment sources given by number of samples and percentages of total samples.

Interpretation	n	Percentage
old creek sediment	6	4%
river sediment	30	19%
reworked polder sediment	25	16%
river sediment / man-made reworked sediment	4	3%
reworked polder sediment/ man-made reworked sediment	66	43%
old creek sediment/ reworked polder sediment	23	15%

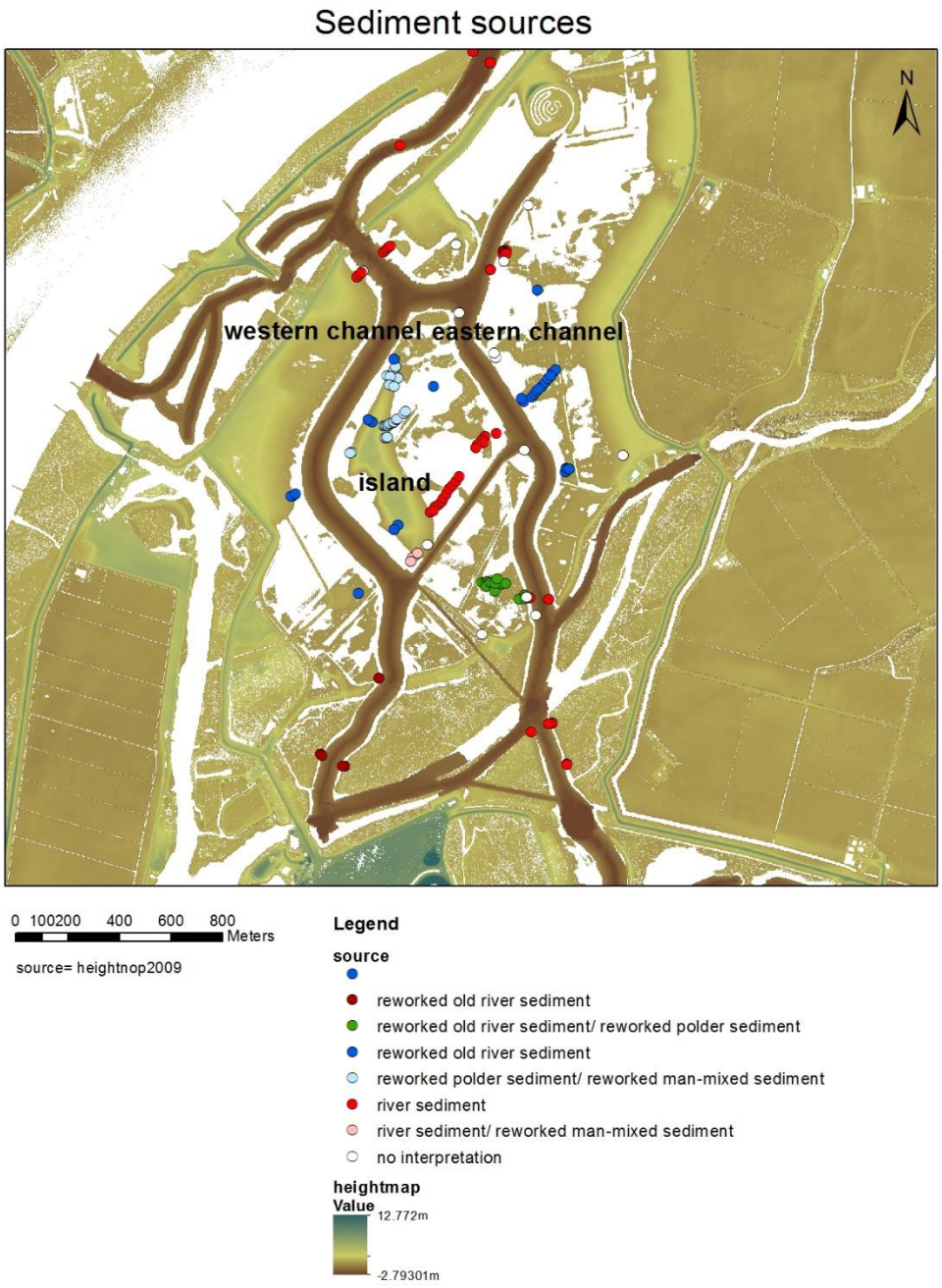

Figure 17. Sediment sources projected on height map.

6 Conclusions

To conclude. A difference in composition of the sediment was found in terms of the zinc concentration normalized by rubidium concentration. Due to this difference in composition, two sources could be predicted and calculated: river and polder originated sediment. When quantifying the first fingerprint technique, it comes down to the fact that of the freshly deposited sediment in the area, 43 % originated from the river versus 57 % of the deposited sediment which originated from the polder itself.

The variance of the calculations for the weighted ratio is 0.0074. The unknown original composition of the sediment causes for 86 ± 38% of this variance and the regression analysis causes for 14 ± 38%.

The freshly deposited sediment thickness varied in the study area from 0 to 11.5 cm but the varying was as well on the small spatial scale as the larger spatial scale.

Further research in the history of the study area has led to even more possible sources: firstly, the river sediment since it has an increased zinc concentration due to stream-upwards pollution. Secondly, the reworked polder sediment because of its relatively low zinc concentrations. Thirdly, the reworked old tidal creek sediment because they have very high zinc concentrations as result of large zinc peaks in the water and sediment in the river Meuse and Rhine in the 1930s and 1960s. Lastly, while adapting the former polder to a natural wetland, human building activities led to a man-made sediment with which the island and some grassland were elevated. The erosion of these elevated parts of the study area provides evidence for the last source of the sediment in the study area: the reworked man-made sediment.

The distribution of the sediment varies locally, near to the inlet of the study area, most sediment originated from the river, further downstream the polder sediment is reworked and most downstream a mixed of the river sediment and reworked polder sediment is found. In the middle of the study area the sedimentation rates are relative higher than at the outer parts of the area. Near the tidal creek in the south higher zinc values are found indicating more contaminated sediment. Around the island in the middle of the area, man-made sediment is reworked and deposited.

7 Bibliography

7.1 Reference list

Anonymous. (1994). *Evaluatienota water 1993: Regeringsbeslissing: Aanvullende beleidsmaatregelen en financiering 1994-1998.* the Haque: Directorate General for Public Works and Water Management RIZA and DGW.

Asselen, v. S. (2010). Peat compaction in deltas: implications for Holocene delta evolution. *Netherlands Geographical Studies 395*, PhD thesis.

Barendregt, A., Baldwin, A. B., & Whigham, D. (2009). *Tidal freshwater wetlands, an introduction to the ecosystem.* Leiden: Backhuys Publishers.

Beck, H. L. (1974). Gamma radiation from radon daughters in the atmosphere. *Geophys. Res. 79*, p. 2215-2221.

Bianchi, T. S., & Allison, M. A. (2009). Large-river delta-front estuaries as natural recorders of global environmental change. *PNAS vol.106 no20*, p. 8085-8092.

Bianchi, T. S., Allison, M. A., & Cai, W. (2013). *Biogeochemical dynamics at major river-coastal interfaces, linkages with global change.* Cambridge: Cambridge University Press.

Bierman, P. R., Albrecht, A., Bothner, M. H., Brown, E. T., Bullen, T. D., Gray, L. B., & Turpin, L. (1998). Erosion, weathering and sedimentation. *Plant physiology 36*, p. 133-138.

Busschers, F. H., Weerts, H. J., Wallings, J., Kasse, C., Cleveringa, P., de Wolf, H., & Cohen, K. M. (2005). Sedimentary architecture and optical dating of Middle and Late Pleistocene Rhine-Meuse deposits - fluvial response to climate change, sea-level fluctuation and glaciation. *Netherlands journal of Geosciences/ Geologie en Mijnbouw 84*, p. 25 - 41.

Collins, A. L., & Walling, D. E. (2002). Selecting fingerprinting properties for discriminating potential suspended sediment sources in river basins. *Journal of hydrology 261,*, p. 218-244.

Collins, A., Walling, D., & Leeks, G. (1988). use of composite fingerprinting to determine the provenance of the contemporary suspended sediment load transported by rivers. *earth surface processes and landforms, 23*, p31-52.

de Boois, H. (1982). Veranderingen in het milieu en de vegetatie in de Biesbosch door de afsluiting van het Haringvliet. *Wageningen University and Research Center (In Dutch, with English summary).*

Dypvik, H., & Harris, N. B. (2001). Geochemical facies analysis of fine-grained siliciclastics using. *Chemical Geology 181*, p. 131–146.

Forstner, U., & Salomons, W. (1980). Trace metal analysis on polluted sediments. *Environmental Technology Letters 1*, p. 494-505.

Hebink, K., Middelkoop, H., Van Diepen, N., Van der Graaf, E. R., & de Meijer, R. (2007). Radiometric fingerprinting of fluvial sediments in the Rhine-Meuse delta, the Netherlands – a feasibility test. *Netherlands Journal of Geosciences Geologie en Mijnbouw 86-3*, p. 229-240.

Kleinhans, M. W., Weerts, H. J., & Cohen, K. M. (2010). Avulsion in action: Reconstruction and modelling sedimentation pace and upstream flood water levels following a Medieval tidal-river diversion catastrophe (Biesbosch, The Netherlands, 1421–1750 AD). *Geomorphology 118*, p. 65-79.

Kumar, A., Kumar, M., Singh, B., & Singh, S. (2003). Natural activities of and in some Indian building materials. *Radiation Measurements, Volume 36, Issues 1–6*, p. 465–469.

Loughran, R. J., Campbell, B. L., & Elliott, G. L. (1982). The identification and quantification of sediment sources using 137Cs. *Appl. Radio. Isor. Vol. 39. No. II*, p. 1153-1157.

Masson, O., Baeza, A., Bieringer, J., Brudecki, K., Bucci, S., Cappai, M., . . . Zhukova, O. (2011). Tracking of Airborne Radionuclides from the Damaged Fukushima. *Environmental science and technology*, p7671-7677.

Matsuura, K., Szöllösi-Nagy, A., Steduto, P., Shamir, U., Ross-Larson, B., & de Coquereaumont, M. (2009). *Water in a changing world.* Istanbul: UNESCO, The United Nations World Water Development Report 3.

Middelkoop, H. (1997). Embanked floodplains in the Netherlands. Geomorphological evolution over various time scales. *Netherlands Geographical Studies 224*, p. 1-352.

Middelkoop, H. (2000). Heavy metal pollution of the river Rhine and Meuse floodplains in the Netherlands. *Geologie en Mijnbouw / Netherlands Journal of Geosciences 79 issue 4*, p. 411-428.

Motha, J. A., Wallbrinka, P. J., Hairsinea, P. B., & Grayson, R. B. (2004). Unsealed roads as suspended sediment sources in an agricultural catchment in south-eastern Australia. *Journal of Hydrology 286*, p. 1-8.

mRO. (2015, mai 25th). *Gemeente Werkendam, bestemmingsplan zoetwatergetijdengebied Noordwaard.* Retrieved from file:///C:/Users/nanda/Downloads/BP%20Zoetwatergetijdengebied%20Noordwaard_vastgesteld_toelichting.pdf

Noordwaard, P. (2007). *Ontwerpvisie ontpoldering noordwaard, het regio alternatief.* Rotterdam: Thieme Grafimedia Groep.

Oude Voshaar, J. (1994). *Statistiek voor onderzoekers met voorbeelden uit de landbouw en milieuwetenschappen. .* Wageningen: Wageningen Pers .

Peart , M. R., & Walling, D. E. (1988). Fingerprinting sediment source: The example of a drainage basin. *International Association of Hydrological Sciences Publication No. 174*, p. 269-279.

Peart, M. R., & Walling, D. E. (1982). Particle size characteristics of fluvial suspended sediment. *IAHS Publ. no. 137.*, p. 397-407.

Rijkswaterstaat, D.-I.-D. (2015, 1 22). Retrieved from waterbase: www.live.waterbase.nl

Rijkwaterstaat. (2015, july 8). *Rijkswaterstaat ministerie van infrastructuur en milieu*. Retrieved from nieuwe merwede: http://www.rijkswaterstaat.nl/water/feiten_en_cijfers/vaarwegenoverzicht/nieuwe_merwede/

Smeth, d. J. (2011). Field portable xray fluoresence, possibilities and limitations. *ESA research seminar.* University of Twente.

Steinhauser, G., Merz, S., Hainz, D., & Sterba, J. (2013). Artificial radioactivity in environmental media (air, rainwater, soil, vegetation) in Austria after the Fukushima nuclear accident. *Environmental Science Pollution Research*, p2527- 2534.

Syvitski, J., Kettner, A., Overeem, I., Hutton, E., Hannon, M., Brakenridge, G., & Day, J. (2009). Sinking deltas due to human activities. *Nature Geoscience 2*, p. 681-686.

Syvitski, J., Vörösmarty, C., Green, P., & Kettner, A. (2005). Impacts of humans on the flux of terrestrial sediment to the global coastal ocean. *Science 308 (5720)*, p. 378-380.

Tilburg, H. v. (n.d.). *geschiedenis spieringsluis*. Retrieved from national park biesbosch: http://www.biesbosch.info/geschiedenis.htm

Törnqvist, T., Wallace, D., Storms, J., Blaauw, M., Derksen, M., Klerks, C., . . . van Dam, L. (2008). Mississipi Delta subsidence primarily caused by compaction of Holocene strata. *Nature Geoscience 1*, p. 173-176.

van Aken, J. (2013). *Determination of 210Pb and 137Cs based sedimentation rates.* in preparation.

van der Perk, M. (2012). *Soil and Water contamination, second edition.* M.C Escher company.

Walling, D. (2006). Human impact on land-ocean sediment transfer by the world's rivers. *Geomorphology 79*, p. 192-216.

Walling, D. E., & Collins, A. L. (2002). Selecting fingerprint properties for discriminating potential suspended sediment sources in river basins. *Journal of Hydrology 261*, p. 218- 244.

Zonneveld, I. (1960). De Brabantse Biesbosch. A study of soil and vegetation of a fresh tidal delta. *Verslagen van lanbouwkundige onderzoekingen No. 65.20 (partly in dutch)*.

7.2 Table of figures

7.3 Appendices